



Early season N₂O emissions under variable water management in rice systems: source-partitioning emissions using isotopocule signatures along a depth profile

5 Elizabeth Verhoeven¹, Matti Barthel¹, Longfei Yu², Luisella Celi³, Daniel Said-Pullicino³, Steven Sleutel⁴, Dominika Lewicka-Szczebak⁵, Johan Six¹, Charlotte Decock¹⁶

¹Department of Environmental Systems Science, ETH Zurich, 8092 Zurich, Switzerland

²Department of Air Pollution and Environmental Technology, EMPA, 8600 Dübendorf, Switzerland

³Department of Agricultural, Forest and Food Sciences, University of Turin, 10095 Grugliasco, Italy

10 ⁴Department of Soil Management, Faculty of Bioscience and Engineering, 9000 Ghent University, Belgium

⁵Thünen Institute of Climate-Smart Agriculture, 38116 Braunschweig, Germany

⁶Department of Natural Resources Management and Environmental Sciences, California State University, 93407 San Luis Obispo, California

15 *Correspondence to:* Elizabeth Verhoeven (elizabeth.verhoeven@gmail.com)

Abstract. Soil moisture strongly affects the balance between nitrification, denitrification and N₂O reduction and therefore the nitrogen (N) efficiency and N losses in agricultural systems. In rice systems, there is a need to improve alternative water management practices, which are designed to save water and reduce methane emissions, but may increase N₂O and decrease nitrogen use efficiency. In a field experiment with three water management treatments, we measured N₂O isotopocule signatures ($\delta^{15}\text{N}$, $\delta^{18}\text{O}$ and site preference, *SP*) of emitted and pore air N₂O over the course of six weeks in the early rice growing season. Isotopocule measurements were coupled with simultaneous measurements of pore water NO₃⁻, NH₄⁺, dissolved organic carbon (DOC), water filled pore space (WFPS) and soil redox potential (Eh) at three soil depths. We then used the relationship between *SP* x $\delta^{18}\text{O}$ -N₂O and *SP* x $\delta^{15}\text{N}$ -N₂O in simple two endmember mixing models to evaluate the contribution of nitrification, denitrification, fungal denitrification to total N₂O emissions and to estimate N₂O reduction rates. N₂O emissions were higher in a dry-seeded + alternate wetting and drying (DS-AWD) treatment relative to water-seeded + alternate wetting and drying (WS-AWD) and water-seeded + conventional flooding (WS-FLD) treatments. In the DS-AWD treatment the highest emissions were associated with a high contribution from denitrification and a decrease in N₂O reduction; while in the WS treatments, the highest emissions occurred when contributions from denitrification/nitrifier-denitrification and nitrification/fungal denitrification were more equal. Modeled denitrification rates appeared to be tightly linked to nitrification and NO₃⁻ availability in all treatments, thus water management affected the rate of denitrification and N₂O reduction by controlling the substrate availability for each process (NO₃⁻ and N₂O), likely through changes in mineralization and nitrification



rates. Our model estimates of mean N_2O reduction rates match well those observed in ^{15}N fertilizer labeling studies in rice systems and show promise for the use of dual isotopocule mixing models to estimate N_2 losses.

1 Introduction

Atmospheric nitrous oxide (N_2O) concentrations continue to rise, and with a global warming potential 298 times that of CO_2 , N_2O is a significant contributor to global warming (IPCC, 2007; Ravishankara *et al.*, 2009). Agriculture is estimated to be responsible for roughly 60% of anthropogenic N_2O emissions (Smith *et al.*, 2008). Considering this, the quantification of field scale N_2O emissions has been the focus of many studies in the last decades and much progress has been made on identifying agricultural management practices, soil and climate variables that influence emissions (Mosier *et al.*, 1998; Venterea *et al.*, 2012; Verhoeven *et al.*, 2017). However, it remains difficult to quantitatively determine the biological sources of emitted N_2O in the field, and knowledge gaps remain in our understanding of how N_2O production and reduction processes change with both time and depth. More specific knowledge of process dynamics is therefore needed to inform and improve biogeochemical models.

N_2O is predominately produced 1) as a byproduct during nitrification, where NH_4^+ is oxidized to NO_3^- via hydroxylamine (NH_2OH); this step of nitrification is sometimes referred to as hydroxylamine oxidation (Schreiber *et al.*, 2012; Hu *et al.*, 2015) or 2) as an intermediate in the denitrification pathway during which NO_3^- is reduced to N_2 (Firestone *et al.*, 1989) or 3) during nitrifier-denitrification by specific ammonia oxidizing bacteria that oxidize NH_4^+ to NH_2OH and then to NO_2^- , with a small fraction of NO_2^- then being reduced to NO and N_2O (Wrage *et al.*, 2001; Kool *et al.*, 2010; Kool *et al.*, 2011). N_2O may also be produced from additional biotic and abiotic processes, such as fungal denitrification, coupled nitrification-denitrification, dissimilatory nitrate reduction to ammonium, chemodenitrification or hydroxylamine decomposition (Butterbach-Bahl *et al.*, 2013; Heil *et al.*, 2015; Zhu-Barker *et al.*, 2015). Due to the prevalence of anaerobic conditions and the use of NH_4^+ based fertilizers fungal denitrification and coupled nitrification-denitrification, respectively, are likely to increase in flooded rice systems. N_2O is consumed during the final step of denitrification, where N_2O is reduced to N_2 by the N_2O reductase pathway. This can occur sequentially within denitrifying organisms, or N_2O produced elsewhere from other processes or incomplete denitrification can be later reduced by denitrifiers. The final and dominant product of denitrification is N_2 . While, N_2 emissions are not of concern for global warming, the quantification of gross denitrification rates is of environmental concern because the loss of N via this process may represent a loss of N from system and indicate reduced fertilizer N efficiency. Gross denitrification rates are difficult to measure *in situ* without the use of isotope tracers due to the high atmospheric background of N_2 , thus denitrification and N_2 emissions remain a relatively unconstrained aspect of N budgets.

Studying N cycling in rice systems offers a unique opportunity to study processes of N_2O production and reduction. Firstly, the complex hydrology, and variable soil moisture conditions between soil layers and within the time course of a growing



season, may induce a patchwork of conditions favorable for nitrification versus denitrification versus N_2O reduction. For example, it is not clear if low N_2O emissions under more moist conditions are the result of lower N_2O production due to substrate limitation (i.e. low nitrification rates and hence low NO_3^-) or rather increased N_2O reduction. To date, few studies have looked at N_2O processes at depth and it is not known how moisture and nutrient stratification affect the balance between

5 N_2O production and consumption processes and ultimately surface emissions. Analysis of soil N_2O concentrations along a profile should help answer this. Secondly, there is a strong need to develop alternative water management practices with shortened paddy flooding period, in order to save water and mitigate methane (CH_4) emissions. However, such systems can cause an increase in N_2O emission that may partially offset the decrease in CH_4 emission (Devkota *et al.*, 2013; Xu *et al.*, 2015; Miniotti *et al.*, 2016). Hence, water management practices should be improved based on a better understanding of the

10 spatiotemporal origin of N_2O emissions and inorganic N precursors, nitrate and ammonium. Thirdly, rice cropping systems typically suffer from a lower nitrogen use efficiency (NUE) than other major cereal crops, often attributed to high gaseous NH_3 and N_2 losses (Dedatta *et al.*, 1991; Cassman *et al.*, 1998; Aulakh *et al.*, 2001; Dong *et al.*, 2012). In improving the NUE, a better estimate of N_2O reduction to N_2 is needed to design strategies that reduce N_2 losses without increasing N_2O emission.

15 The measurement of N_2O isotope signatures at natural abundance is a tool to differentiate between *in situ* N_2O source processes and N_2O reduction (Baggs, 2008; Ostrom and Ostrom, 2011; Toyoda *et al.*, 2011; Wolf *et al.*, 2015), i.e. N_2O source-partitioning. The evolution of analytical techniques now allows us to measure not only the bulk $\delta^{15}\text{N}$ - N_2O , but also the intermolecular distribution of the $\delta^{15}\text{N}$ within N_2O , called site-preference (SP) and the $\delta^{15}\text{N}$ of N_2O precursors, nitrate (NO_3^-) and ammonium (NH_4^+). The $\delta^{18}\text{O}$ of N_2O and its precursors may also be used to constrain processes (Kool *et al.*, 2009;

20 Lewicka-Szczebak *et al.*, 2016; Lewicka-Szczebak *et al.*, 2017). Analytical methods of interpretation remain, however, only semi-quantitative due to uncertainty surrounding net isotope effects (ϵ) for individual processes, overlap in the δ signatures between processes, and/or multiple N and O sources for which determination of $\delta^{15}\text{N}$ and $\delta^{18}\text{O}$ remains expensive and time consuming. Theoretically, the O in N_2O derives from O_2 during nitrification and from NO_3^- during denitrification or a combination during nitrifier-denitrification (Kool *et al.*, 2007; Kool *et al.*, 2010; Snider *et al.*, 2012, 2013; Lewicka-Szczebak

25 *et al.*, 2016). However, in the case of nitrifier-denitrification and denitrification, intermediates in the reduction pathway (NO_2^- and NO) can extensively exchange O atoms with H_2O (Kool *et al.*, 2007). Such exchange lowers the measured $\delta^{18}\text{O}$ - N_2O values because the influence of relatively depleted $\delta^{18}\text{O}$ from H_2O , potentially leading to an underestimation of denitrification and N_2O reduction (Snider *et al.*, 2013; Lewicka-Szczebak *et al.*, 2016). Indeed, it has been shown that the $\epsilon^{18}\text{O}$ for denitrification should be calculated relative to H_2O not NO_3^- , as almost 100% O exchange occurs (Lewicka-Szczebak *et al.*,

30 2014; Lewicka-Szczebak *et al.*, 2016). The use of $\delta^{15}\text{N}$ values is theoretically more straightforward and there is also a much richer body of literature on $\epsilon^{15}\text{N}$ for various processes, which was recently compiled and reviewed by Denk *et al.* (2017). The authors report a mean isotope effect for ^{15}N during NH_4^+ oxidation to N_2O of $-56.6 \pm 7.3\text{‰}$ and of $-42.9 \pm 6.3\text{‰}$ for NO_3^- reduction to N_2O . Additionally, accurate measurement of the $\delta^{15}\text{N}$ of NH_4^+ and NO_3^- at sufficient temporal resolution remains time consuming. In comparison, the SP is thought to be independent of the initial substrate $\delta^{15}\text{N}$ values and shows distinct



values for two clusters of N_2O production, namely $32.8 \pm 4.0\%$ for nitrification/fungal denitrification/abiotic N_2O production and $-1.6 \pm 3.8\%$ for denitrification/nitrifier-denitrification (Decock and Six, 2013a; Denk *et al.*, 2017).

All three δ values are affected by N_2O reduction to N_2 , which serves to enrich in heavy isotopes (^{15}N and ^{18}O) the pool of remaining N_2O that is measured (Decock and Six, 2013a; Zou *et al.*, 2014). If the δ value of $\text{N}_2\text{O}_{\text{initial}}$ (prior to reduction) can be reasonably estimated from graphical and mixing model approaches, then the subsequent enrichment of N_2O can be used to estimate N_2O reduction rates and thereby total denitrification rates. This is important because N_2O reduction is a crucial but exceptionally poorly constrained process within the N cycle (Lewicka-Szczebak *et al.*, 2017). Fractionation during N_2O reduction may follow dynamics of open or closed systems (Mariotti *et al.*, 1981; Fry, 2007). In open systems a continuous supply of fresh (and non-enriched) N_2O is assumed to enter the system, while in closed systems a given pool of N_2O is progressively used up. Closed system dynamics result in a greater enrichment of the residual N_2O pool and lower associated N_2O reduction rates. In reality *in situ* processes likely exhibit aspects of both systems heterogeneously in time and space (Decock and Six, 2013b).

Our goal was to collect a high resolution *in situ* N_2O isotopocules data set that could be used to a) determine the stratification of N_2O production and reduction processes in relation to water management, b) semi-quantitatively assess N_2O and N_2 losses among rice water management treatments and c) push forward current natural abundance N_2O isotope source-partitioning methods and interpretation at the field scale. We compared three rice water management practices: direct dry seeding followed by alternate wetting and drying (DS-AWD), wet seeding followed by alternate wetting and drying (WS-AWD) and wet seeding followed by conventional flooding (WS-FLD). Isotope data was determined at three depths, simultaneously with soil environmental and nutrient data and soil N_2O and dissolved N_2O concentrations. We hypothesized that N_2O emissions would be highest in the AWD treatments due to greater contributions from nitrification and less N_2O reduction, following the order: DS-AWD > WS-AWD > WS-FLD. We also hypothesized that N_2 emissions are controlled by the availability of NO_3^- coming from nitrification and high soil moisture. We considered that NO_3^- would be higher under WS-AWD but soil moisture would be higher under WS-FLD; therefore we predicted N_2 emissions to follow in the order: WS-AWD > WS-FLD > DS-AWD. Lastly, we hypothesized that longer periods of lowered soil moisture in the DS-AWD and WS-AWD treatments would result in greater production of N_2O at depth and this higher production would increase surface emissions.

2 Materials and Methods

2.1 Field experiment

A field experiment consisting of three water management regimes was conducted at the Italian Rice Research Center (Ente Nazionale Risi), Pavia, Italy ($45^\circ 14' 48''\text{N}$, $8^\circ 41' 52''\text{E}$). Experimental work focused only on the early growing season, lasting



from the 13th of May, 2016 until June 30th, 2016. It is in this period that the highest N₂O losses and N cycling dynamics had been previously observed and the largest differences among water management practices occurred. The experimental platform has been extensively described in previous publications (Miniotti *et al.*, 2016; Peyron *et al.*, 2016; Said-Pullicino *et al.*, 2016; Verhoeven *et al.*, 2018). The soil at the site has been classified as coarse silty, mixed, mesic Fluvaquentic Epiaquept (USDA-NRCS, 2010). The mean soil texture in the upper 30 cm of the experimental plots was 26% sand, 62% silt, and 11% clay with a mean bulk density of 1.29 g cm⁻³. The mean total organic C and total N were 1.07 and 0.11% and pH 5.9 (1:2.5 H₂O) and 5.2 (1:2.5 0.01M CaCl₂), respectively. Annual and growing season mean temperatures in 2016 were 10°C and 23°C, respectively (Fig. S1). Annual and growing season cumulative precipitation was 618 and 258 mm, respectively. Data for both values were retrieved from a regional weather station operated by the Agenzia Regionale per la Protezione dell'Ambiente-Lombardia, located approximately 200 m from the field site (ARPA).

Water management in the two WS treatments was identical during the first three weeks of the growing season (Table 1). Following regional practices for water seeding, paddies were flooded for six days at the time of seeding, but then drained for ~ 2 weeks to promote germination. During this period of 'drainage' paddies were not dry but maintained near saturation by flush irrigation as necessary (May 31st and June 6th). Flush irrigation is a practice in which the water inlet channels are opened for a few hours and then the outlet channels are opened a few hours later resulting in temporary soil saturation or even 1-2 cm ponding for 2-4 hours. On June 10th, approximately three weeks after seeding, treatment differentiation between the WS-FLD and WS-AWD began. At this time the WS-FLD was flooded, while the WS-AWD was only flush irrigated. On June 16th, the WS-FLD was allowed to drain slowly in order to facilitate fertilizer application on June 21st. Following fertilizer application, the WS-FLD treatment was re-flooded and both AWD treatments were flush irrigated on June 22nd. In the DS-AWD treatment no flooding or irrigation water was applied prior to June 22nd. Soil moisture depended on rainfall, which was 75 mm during the four weeks following seeding.

In all treatments, crop residues were incorporated in the spring, before the cropping season. All paddies were harrowed and leveled approximately one month prior to seeding in mid-April, 2016. All treatments were pre-fertilized with phosphorus and potassium on May 13th (14 and 28 kg ha⁻¹, respectively) and with urea on May 16th (40 and 60 kg ha⁻¹ for the DS and WS treatments, respectively). The DS-AWD treatment was seeded on May 17th, 2016. The WS-FLD and WS-AWD treatments were seeded on May 20th. All treatments were fertilized with urea on June 21st (70 and 60 kg ha⁻¹ for the DS and WS treatments, respectively). All treatments were harvested on September 15th.

Each treatment consisted of two paddies, 20 x 80 m, with two plots in each paddy, n=4 (Fig. S2). The experimental design was identical to that of Verhoeven *et al.* (2018), with the addition of the DS-AWD treatment and some adjustment to plot placement in order to accommodate data logging devices and field equipment. Each paddy was approximately 2 m apart and hydrologically separated by a levee of 50 cm above the soil surface, flanked by an irrigation canal on either side. Sampling for N₂O surface fluxes, pore water parameters (NO₃⁻, NH₄⁺, DOC, dissolved N₂O) and pore air N₂O occurred on 15-17 dates,



from the 20th of May to the 30th of June, 2016 (Table S1). Sampling dates were on average three days apart with a greater frequency before and after N application on the 21st of June. Sub-samples of pore water from 10 to 12 dates were analyzed for $\delta^{15}\text{N-NO}_3^-$, $\delta^{18}\text{O-NO}_3^-$ and $\delta^{15}\text{N-NH}_4^+$.

2.2 Soil environment: temperature, redox potential, and moisture

5 Soil moisture was measured using PR2 capacitance probes (Delta T Devices, UK) at 5, 15, 25, 45 and 85 cm. Water filled pore space (WFPS) was calculated using bulk density measurements at 5, 12.5 and 25 cm collected at the beginning of the season using a Giddings manual soil auger. Soil temperature was measured in only one plot per paddy ($n=2$) at three depths (5, 12.5 and 25 cm). Measurements were made manually at the time of surface flux gas measurements. Soil redox potential (Eh) was measured continuously in each plot using sturdy tip probes outfitted with 5 Pt-electrodes that were permanently
 10 connected to a 48-channel Hypnos-III data logger (MVH Consult, The Netherlands) with two Ag/AgCl-reference probes. Soil Eh was measured every hour at six depths; 5, 12.5, 20, 30, 50 and 80 cm. We took the average of the 20 and 30 cm readings to derive a 25 cm reading in order to correlate to other measurements.

2.3 N₂O measurements: surface emissions, pore air, and dissolved gas

All N₂O concentration measurements were measured by gas chromatography on a Scion 456-GC (Bruker, Germany) equipped
 15 with an electron capture detector (ECD). The error of the GC was determined to be ± 0.012 at 0.3 ppm and ± 0.024 ppm at 1.0 ppm. N₂O surface emissions ($\text{N}_2\text{O}_{\text{emitted}}$) were measured by the non-steady state closed chamber technique (Hutchinson and Mosier, 1981). The chamber design and deployment was identical to that of Verhoeven *et al.* (2018). Gas samples were taken at 0, 10, 20 and 30 min in each chamber and injected into pre-evacuated exetainers (Labco, UK). At time 0 and 30 min an additional ~ 170 ml of sample was taken and injected into gas crimp neck vials sealed with Butyl injection stoppers (IVA
 20 Analysentechnik, Germany) to be used for isotope analysis. When the accumulation of gas over the course of measurement was less than the GC error associated with the highest concentration of the four measurements, the flux was set to zero. Fluxes above the detection limit were calculated by linear or non-linear regression following the method outlined by Verhoeven and Six (2014). Soil N₂O ($\text{N}_2\text{O}_{\text{soil}}$) was sampled using passive diffusion probes installed at 5, 12.5 and 25 cm. The probe design and sampling strategy has been previously described in Verhoeven *et al.* (2018). In brief, the samples were collected in He
 25 flushed and pre-evacuated 100 ml glass crimp neck vials (actual volume 110 ml, IVA Analysentechnik, Germany) and after sampling topped with high purity He gas to prevent leakage into under-pressurized vials. The final N₂O concentration was determined by gas chromatography, as described above, on a subsample, while the remainder of the sample was retained for isotope analysis. The final N₂O concentration was calculated by accounting for sample dilution based on the pressure after evacuation, after sampling and after topping with He gas. Samples for dissolved N₂O ($\text{N}_2\text{O}_{\text{dissolved}}$) were collected by injecting
 30 a 5 ml subsample of pore water, collected as described in section 2.4, into N₂ flushed and filled exetainers that also contained 50 μl of 50% ZnCl to stop microbial activity. Samples were stored at 4°C until the end of the experimental campaign and transported back to the lab for analysis, therefore there was adequate time for the equilibration between the headspace and



aqueous phases. The molar concentration of N_2O was calculated by applying the solubility constant of N_2O at the time of analysis (i.e. lab temperature) to Henry's law (Wilhelm *et al.*, 1977; Weiss and Price, 1980; Lide, 2004), taking into account the vial volume and headspace.

2.4 Pore water measurements

Two MacroRhizon pore water samplers (Rhizosphere Research Products, The Netherlands) were installed at each depth (5, 12.5 and 25 cm) in every plot. Pore water was then collected in two polypropylene 60 ml syringes at each depth and later pooled together at sample processing. The syringes were attached to the MacroRhizon sample tubes with two-way leuc lock valves and propped open using a wedge, which served to create a low vacuum; the syringes were left to collect water for 2-4 h. Samples were stored at 4°C and processed within 36 h. During pore water processing ~ 15 ml of solution was allocated for analysis of NO_3^- and NH_4^+ and $\delta^{15}\text{N}$, $\delta^{18}\text{O}-\text{NO}_3^-$, ~ 15 ml for $\delta^{15}\text{N}-\text{NH}_4^+$, 5 ml for dissolved N_2O , 3-5 ml for dissolved Fe^{2+} and Mn^{2+} and 5 ml for DOC/TDN analysis. All samples, aside from those for dissolved N_2O , were frozen at -5°C until analysis. NO_3^- and NH_4^+ were determined by spectrophotometry following the procedure of (Doane and Horváth, 2003). DOC and TDN were determined by first acidifying the water sample to pH <2 by addition of concentrated HCl and then analysis on a multi N/C 2100S:TOC/TN Analyzer (Analytik Jena, Germany).

2.5 Determination of $\delta^{15}\text{N}$, $\delta^{18}\text{O}$ and isotopomer signatures in $\text{N}_2\text{O}_{\text{emitted}}$ and $\text{N}_2\text{O}_{\text{soil}}$

Surface and pore air gas samples were taken in 100 ml glass crimp neck vials (actual volume 110 ml, IVA Analysentechnik, Germany) as described in section 2.3. Pore air gas samples were preconditioned with 1ml of 1M NaOH solution prior to analysis due to very high CO_2 concentrations in many samples (> 5000 ppm). The intramolecular site-specific isotopic composition of the N_2O molecule was measured using a gas preparation unit (Trace Gas, Elementar, UK) coupled to an isotope ratio mass spectrometer (IRMS; IsoPrime100, Elementar, UK). The gas preparation unit was modified with an additional chemical trap ($\frac{1}{2}$ " diameter stainless steel), located immediately downstream from the autosampler. This pre-trap was filled with NaOH, $\text{Mg}(\text{ClO}_4)_2$, and activated carbon in the direction of flow and is designed to further scrub CO_2 , H_2O , CO and VOCs which otherwise would cause mass interference during measurement. Before final injection into the IRMS the purified gas sample is directed through a Nafion drier and subsequently separated in a gas chromatograph column (5Å molecular sieve). The IRMS consists of five Faraday cups with m/z of 30, 31, 44, 45, 46, measuring $\delta^{15}\text{N}$ and $\delta^{18}\text{O}$ of N_2O and $\delta^{15}\text{N}$ from the NO^+ fragments dissociated from N_2O during ionization in the source. The $^{15}\text{N}/^{14}\text{N}$ ratio of the NO molecule is used to calculate the α (central) position of the initial N_2O , thus allowing measurement of the site-specific isotopic composition of N_2O (SP). Site preference is defined as $\delta^{15}\text{N}^{\text{SP}} = \delta^{15}\text{N}^{\alpha} - \delta^{15}\text{N}^{\beta}$ with α denoting the $^{15}\text{N}/^{14}\text{N}$ ratio of the central N atom and β the $^{15}\text{N}/^{14}\text{N}$ ratio of the terminal N atom of the linear NNO molecule. $\delta^{15}\text{N}^{\beta}$ is indirectly obtained from rearrangement of:

$$\delta^{15}\text{N}^{\text{bulk}} = (\delta^{15}\text{N}^{\alpha} + \delta^{15}\text{N}^{\beta})/2$$



which represents the average ^{15}N content of the N_2O molecule.

For IRMS calibration three sets of two working standards (~ 3 ppm N_2O mixed in synthetic air) with different isotopic composition ($\delta^{15}\text{N}^\alpha = 0.954 \pm 0.123$ ‰ and 34.446 ± 0.179 ‰; $\delta^{15}\text{N}^\beta = 2.574 \pm 0.086$ ‰ and 35.98 ± 0.221 ‰; $\delta^{18}\text{O} = 39.741 \pm 0.051$ ‰ and 38.527 ± 0.107 ‰) were used. These standards have been analyzed at EMPA using TREX-QCLAS versus standards with assigned δ -values by Tokyo Institute of Technology (Mohn *et al.*, 2014). These working standards were run in triplicate, evenly spaced throughout a run. Sample peak ratios are initially reported against a N_2O reference gas peak (100% N_2O , Carbagas, Switzerland) and are subsequently corrected for drift and span using the working standards. Further correction procedures, such as ^{17}O mass overlap and scrambling, as reported elsewhere, were not applied as the data was inherently corrected by regression between true and measured values of the triplicate working standards. Long-term measurement quality was ensured using a control standard at low N_2O concentration (~ 0.4 ppm) treated as a sample. Instrument linearity and stability was frequently checked by injection of 10 reference gas pulses of either varying or identical height respectively, with accepted levels of $<0.03\%$ /nA. Since instrument linearity could only be achieved for either N_2O or NO, the instrument had been tuned for the former and $\delta^{15}\text{N}^\alpha$ subsequently corrected using sample peak height assuming a non-linearity of 0.1 ‰ nA^{-1} . Such linearity complications have been previously reported using Elementar (Ostrom *et al.*, 2007) and ThermoFinnigan IRMS (Röckmann *et al.*, 2003). Tropospheric air was regularly measured ($n=42$) and used as a confirmation of correction procedures, yielding consistent and reliable results: $\delta^{15}\text{N}^{\text{SP}} = 18.77 \pm 1.08$ ‰; $\delta^{15}\text{N}^{\text{bulk}} = 5.96 \pm 0.35$ ‰; $\delta^{15}\text{N}^\alpha = 15.34 \pm 0.70$ ‰, $\delta^{15}\text{N}^\beta = -3.43 \pm 0.60$ ‰; $\delta^{18}\text{O} = 43.67 \pm 0.41$ ‰. All $^{15}\text{N}/^{14}\text{N}$ sample ratios are reported relatively to the international isotope ratio scale AIR-N2 while $^{18}\text{O}/^{16}\text{O}$ are reported versus Vienna Standard Mean Ocean Water (V-SMOW). Relative differences are given using the delta notation (δ) in units of ‰:

$$\delta^Z X [\text{‰}] = \frac{R_{\text{sample}}}{R_{\text{reference}}} - 1 \quad (1)$$

where R is referring to the molar ratio of $^{15}\text{N}/^{14}\text{N}$ or $^{18}\text{O}/^{16}\text{O}$ and $^Z X$ to the abundance of the heavy stable isotope Z of element X .

2.6 Determination of $\delta^{15}\text{N}\text{-NO}_3^-$, $\delta^{18}\text{O}\text{-NO}_3^-$ and $\delta^{15}\text{N}\text{-NH}_4^+$

Pore water NO_3^- samples were analyzed for $\delta^{15}\text{N}$ and $\delta^{18}\text{O}$ at the University of California, Davis, Stable Isotope Facility (<http://stableisotopefacility.ucdavis.edu/>), using the denitrifier method developed by (Sigman *et al.*, 2001; Casciotti *et al.*, 2002; McIlvin and Casciotti, 2011). $\delta^{15}\text{N}\text{-NH}_4^+$ in pore water was determined by micro-diffusion onto acidified disks followed by persulfate digestion (Stephan and Kavanagh, 2009; Lachouani *et al.*, 2010) and lastly by the denitrifier method. For $\delta^{15}\text{N}\text{-NH}_4^+$, all steps and analyses were done in-house, including the denitrifier method. Briefly, samples were run in sets of 40 with 24 samples and a combination of 16 standards and blanks. Each run contained at least two $\delta^{15}\text{N}\text{-NH}_4^+$ isotope standards (IAEA N2 = 20.3‰; IAEA N1 = 0.4‰; USGS 25 = -30.4‰) at two or three concentrations in duplicate or triplicate in addition to



two blanks and two working standards. NH_4^+ isotope standards were diffused, digested and run through the denitrifier method in parallel with samples and therefore an overall correction and concentration offset was derived and applied for each batch. The denitrifier method was executed using the updated protocol described by McIlvin and Casciotti (2011) using *Pseudomonas aureofaciens* (ATCC 13985). An IAEA KNO_3^- standard ($\delta^{15}\text{N} = 4.7\text{‰}$) was included at the denitrifier method step to ensure accurate conversion of NO_3^- to N_2O . A propagated error across all steps of $\delta^{15}\text{N}\text{-NH}_4^+$ quantification was calculated from the working standards included in each batch ($n=18$). We excluded three values that were well outside the expected range; our overall precision was 1.9‰. The largest sources of error were incomplete diffusion or persulfate digestion. For $\delta^{15}\text{N}\text{-NO}_3^-$ and $\delta^{18}\text{O}\text{-NO}_3^-$ analyzed at SIF, UC-Davis, the limit of quantification was $2.0\text{ }\mu\text{M NO}_3^-$ or $0.125\text{ mg L}^{-1}\text{ NO}_3^-$, with a precision of 0.4‰ and 0.5‰ for $\delta^{15}\text{N}$ and $\delta^{18}\text{O}$, respectively.

The net isotope effect (ϵ) of NO_3^- reduction to N_2O and for NH_4^+ oxidation to N_2O and were calculated using equation 2 and 3, respectively.

$$\epsilon^{15}\text{N}_{\text{N}_2\text{O}-\text{NO}_3} = \delta^{15}\text{N}_{\text{N}_2\text{O}} - \delta^{15}\text{N}_{\text{NO}_3} \quad (2)$$

$$\epsilon^{15}\text{N}_{\text{N}_2\text{O}-\text{NH}_4} = \delta^{15}\text{N}_{\text{N}_2\text{O}} - \delta^{15}\text{N}_{\text{NH}_4} \quad (3)$$

2.7 Determination of N_2O source contribution and N_2O reduction

2.7.1 Two endmember mixing models using SP and $\delta^{18}\text{O}$ signatures: closed and open systems

We tested two mixing models where N_2O reduction was modeled under ‘open’ and ‘closed’ system dynamics following the theory outlined originally by Fry (2007) and Mariotti *et al.* (1981), respectively. The two modelling methods are henceforth referred to as ‘open’ and ‘closed’. Additionally, we modeled two possible scenarios, as described by Lewicka-Szczebak *et al.*, (2017); scenario 1 (sc1), where N_2O is produced and reduced by denitrifiers before mixing with N_2O derived from nitrification or scenario two (sc2) where N_2O is produced from both processes, mixed, and then reduced. In both models, N_2O is originally produced from two possible endmembers; denitrification/nitrifier-denitrification (denoted by subscript *den*) and nitrification/fungal denitrification (denoted by subscript *nit*). In each model we used identical SP endmember values (SP_{den} and SP_{nit}) and N_2O reduction isotope effects ($\epsilon\text{SP}_{\text{red}}$ and $\epsilon^{18}\text{O}_{\text{red}}$) as those compiled in (Lewicka-Szczebak *et al.*, 2017) (Table 2). For the $\delta^{18}\text{O}\text{-N}_2\text{O}_{\text{den}}$, the value used in Lewicka-Szczebak *et al.* (2017) was originally reported relative to the $\delta^{18}\text{O}\text{-H}_2\text{O}$ (as $\delta^{18}\text{O}\text{-N}_2\text{O}(\text{N}_2\text{O}/\text{H}_2\text{O})$). As we did not measure $\delta^{18}\text{O}\text{-H}_2\text{O}$ in our samples, we reported and used our sample $\delta^{18}\text{O}\text{-N}_2\text{O}$ values as is and then corrected the denitrification isotope signature, $\delta^{18}\text{O}\text{-N}_2\text{O}(\text{N}_2\text{O}/\text{H}_2\text{O})_{\text{den}}$, reported by Lewicka-Szczebak *et al.* (2017) by an assumed $\delta^{18}\text{O}\text{-H}_2\text{O}$ of water for our site. We used a $\delta^{18}\text{O}\text{-H}_2\text{O}$ value of -8.3‰ , as reported by Rapti-Caputo and Martinelli (2009) for an uncontained aquifer of the Po River delta. For the $\delta^{18}\text{O}\text{-N}_2\text{O}_{\text{nit}}$ we re-calculated the mean from the six studies used in Lewicka-Szczebak *et al.* (2017), using the original values reported as $\delta^{18}\text{O}\text{-N}_2\text{O}$ (as opposed to $\delta^{18}\text{O}\text{-N}_2\text{O}(\text{N}_2\text{O}/\text{H}_2\text{O})$), this yielded a mean of 36.5‰ (Sutka *et al.*, 2006; Sutka *et al.*, 2008; Frame and Casciotti, 2010; Heil *et al.*, 2014; Rohe *et al.*, 2014; Maeda *et al.*, 2015).



Closed system fractionation for N₂O reduction was modeled following the method described in Lewicka-Szczebak *et al.* (2017) (Fig.1). Here, sample SP and δ¹⁸O-N₂O values are used to derive sample specific intercepts that pass through the sample and reduction line (sc1) or the sample and the mixing line (sc2). A fixed slope for the reduction line can be calculated from εSP_{red} / ε¹⁸O_{red} (i.e. in our case, -5/-15). In sc1, the intercept of the mixing and reduction line represents N₂O that has been produced from denitrification/nitrifier-denitrification and partially reduced but not yet mixed with N₂O produced from nitrification/fungal denitrification. In sc2, the intercept of these lines represents N₂O that has been produced by the two endmember pools, mixed, but not yet reduced. The Y axis (i.e. SP) value of these respective intercepts can be used in a generalized Rayleigh equation (Eq. 4) to calculate the extent of N₂O reduction, represented by the fraction of residual N₂O not reduced.

$$SP_{resid.N_2O} \approx SP_{N_2O-unreduced} + \varepsilon SP_{red} \cdot \ln(rN_2O_{net}) \quad (4)$$

In sc1 the *r*N₂O is determined with respect to N₂O from denitrification/nitrifier-denitrification only, therefore to calculate the residual fraction of total production (i.e. N₂ + N₂O) we calculate gross *r*N₂O:

$$gross\ rN_2O_{sc1} = \frac{1}{\frac{fracDenit_{net}/rN_2O_{net}}{+1-fracDenit_{net}}} \quad (sc1, \text{ in } sc2\ rN_2O_{net} = rN_2O_{gross}) \quad (5)$$

To calculate the fraction of denitrification of the total initially produced N₂O (emitted as N₂O and N₂) we calculate the gross denitrification fraction:

$$gross\ frac_{DEN\ sc1-closed} = \frac{fracDenit_{net}/rN_2O_{net}}{fracDenit_{net}/rN_2O_{net} + 1 - fracDenit_{net}} \quad (sc1) \quad (6)$$

To calculate the fraction of denitrification/nitrifier-denitrification to the net N₂O produced, we use Eq. 7. For simplicity and comparison with open system calculations, we call this *DenContribution*.

$$net\ frac_{DENsc1-closed} = \frac{SP_{sample} - SP_{nit}}{SP_{resid.N_2O} - SP_{nit}} \quad (sc1) = DenContribution_{closed-sc1} \quad (7)$$

In this case, SP_{resid.N₂O} is the signature of residual bacterial N₂O after partial reduction but before mixing. This was determined from the graphical method (Lewicka-Szczebak *et al.*, 2017). In sc2 both net and gross fractions of denitrification are equal and can be expressed as:

$$DenContribution_{closed-sc2} = \frac{SP_{N_2O-unreduced} - SP_{nit}}{SP_{den} - SP_{nit}} \quad (sc2) \quad (8)$$

Here, SP_{N₂O-undreduced} is the signature of N₂O mixed from nitrification/fungal denitrification and denitrification/nitrifier-denitrification, but before reduction. This was determined from the graphical method (Lewicka-Szczebak *et al.*, 2017).

To predict *r*N₂O in open systems we set up a series of mass balance equations using our measured N₂O flux or N₂O_{poreair} concentrations and measured δ¹⁸O and SP values. We used the same endmember values listed in Table 2 for all equations. As above, we can model the interaction between mixing and reduction assuming sc1 (Eqs 9-11) or sc2 (Eqs 9,12,13). In Eqs 9-13, we use *k*_{nitr}, *k*_{den} and *k*_{red} to represent the gross process rates or concentrations of N₂O attributable to nitrification, denitrification and N₂O reduction, respectively.



$$N_2O_{flux}(or\ N_2O_{poreair}) = k_{nit} + k_{den} - k_{red} \quad \text{note: } k_{den} = \text{total denitrification (N}_2\text{O} + \text{N}_2) \quad (9)$$

$$SP - N_2O_{measured} = \frac{SP_{nit}k_{nit} + \left(SP_{den} - \varepsilon SP_{red} \left(\frac{k_{red}}{k_{den}} \right) \right) (k_{den} - k_{red})}{k_{nit} + k_{den} - k_{red}} \quad (sc1) \quad (10)$$

$$\delta^{18}O - N_2O_{measured} = \frac{(\delta^{18}ON_2O_{nit})k_{nit} + \left(\delta^{18}ON_2O_{den} - \varepsilon^{18}O_{red} \left(\frac{k_{red}}{k_{den}} \right) \right) (k_{den} - k_{red})}{k_{nit} + k_{den} - k_{red}} \quad (sc1) \quad (11)$$

$$SP - N_2O_{measured} = \frac{(SP_{nit}k_{nit} + SP_{den}k_{den})}{k_{nit} + k_{den}} - \varepsilon SP_{red} \left(1 - \frac{N_2O_{flux}}{k_{nit} + k_{den}} \right) \quad (sc2) \quad (12)$$

$$5 \quad \delta^{18}O - N_2O_{measured} = \frac{(\delta^{18}ON_2O_{nit})k_{nit} + (\delta^{18}ON_2O_{den})k_{den}}{k_{nit} + k_{den}} - \varepsilon^{18}O_{red} \left(1 - \frac{N_2O_{flux}}{k_{nit} + k_{den}} \right) \quad (sc2) \quad (13)$$

These two sets of equations (Eq. 9,10,11) or (Eq. 9,12,13), representing each scenario, were applied to measured surface fluxes to produce process rates in g N₂O-N ha⁻¹ d⁻¹ or were applied to N₂O_{poreair} concentrations to produce concentrations of N₂O in µg N₂O-N L⁻¹. By rearranging these process rates or concentrations we can calculate gross *r*N₂O, *frac*_{DEN} and the contribution of denitrification to N₂O using Eqs. 14-16.

$$10 \quad \text{gross } \text{frac}_{DEN\ sc1,sc2-open} = \frac{k_{den}}{k_{nit} + k_{den}} \quad (14)$$

$$\text{gross } rN_2O_{sc1,sc2-open} = \frac{k_{nit} + k_{den} - k_{red}}{k_{nit} + k_{den}} \quad (15)$$

$$\text{DenContribution}_{sc1,sc1-open} = \frac{(k_{den} - k_{red})}{[N_2O]}, \quad [N_2O] = N_2O_{flux} \text{ Or } N_2O_{poreair} \quad (16)$$

Plausible solutions for *k*_{red}, *k*_{den}, and *k*_{red} were estimated based on minimizing the sum of squares between the modeled and measured N₂O flux (or concentration), δ¹⁸O and SP values using a Generalized Reduced Gradient (GRG) nonlinear algorithm in the *Solver* function of excel. Solutions with a minimum sum of squares over 500 were considered implausible (8.3% of solutions) (Table S2). Both models produced some non-plausible solutions, i.e. fractional contributions over 1 or under 0. Only solutions with a gross *r*N₂O, gross *frac*_{DEN} and DenContribution between 0 to 1 and an open system minimum sum of squares < 500 were retained. In sc1, roughly 75% of solutions met these criteria. For sc2, less than 10% of solutions in the open system met this criteria, therefore we do not proceed to analyze and discuss solutions from sc2 (Table S2 and Fig. S3).

20 2.8 Statistical analyses

Response variables were analyzed using a linear mixed effects ANCOVA model with treatment, date, and depth (if applicable) as fixed effects and plot as a random effect. The longitudinal position in the field (Y position) measured in meters from the central driveway (Fig. S2), was used as a covariate to account for potential heterogeneity in the longitudinal direction. In the case of non-normally distributed data, data was transformed to obtain a normal distribution of residuals. Due to the non-normal distribution of many variables, Spearman correlations were used to analyze the relationship between N₂O_{emitted} fluxes, isotopocule values, soil environmental and substrate variables. Post-hoc analysis of treatment and depth within a given day was performed using the *lsmeans* function with a Tukey adjustment for multiple comparisons. For the analysis of modeling results we eliminated the 25 cm depth due to poor data availability. All data analysis was done in R version 3.3.2.



3 Results

3.1 N₂O fluxes, dissolved and pore air N₂O concentrations

3.1.1 Temporal patterns in N₂O fluxes and concentrations

After the first basal fertilization (May 16th) and prior to the second topdressing fertilization (June 21st), emissions were significantly higher in the DS-AWD treatment than in WS-AWD and WS-FLD on eight and six of the 11 sampling days, respectively (Fig. 2). During this time four peaks in emissions were observed in the DS-AWD treatment, on May 20th, June 1st-3rd, June 7-9th, and June 20th, averaging 39.5 ± 5.1 g N₂O-N ha⁻¹ d⁻¹. A peak in emissions following the second fertilization (June 21st) was observed in all treatments; in the DS-AWD treatment emissions peaked at 108.2 ± 4.2 g N₂O-N ha⁻¹ d⁻¹ on June 23rd, while in the WS-AWD and WS-FLD treatments, emissions peaked one day earlier reaching 49.4 ± 17.9 and 77.67 ± 10.6 g N₂O-N ha⁻¹ d⁻¹, respectively. In the WS-AWD treatment, emissions remained slightly elevated following this fertilization until the end of the monitoring campaign, while in the DS-AWD and WS-FLD, emissions declined after June 22 or 23rd, respectively.

If we exclude N₂O_{dissolved} measurements from the DS-AWD treatment following the second fertilization (i.e. after the 22nd of June, when concentrations reached as high as 594.4 ± 112.6 µg N₂O-N L⁻¹ at 5 cm), concentrations throughout the profile of all treatments remained under 20 µg N₂O-N L⁻¹. Due to the large differences between dates and treatments we present the concentrations on a log₁₀ scale (Fig. 2) and non-transformed scale (Fig. S4). Peak concentrations in the WS treatments occurred at 5 cm on the first day of measurement, reaching 17.7 ± 5.1 and 18.5 ± 2.8 µg N₂O-N L⁻¹ in the WS-AWD and WS-FLD, respectively. In comparison, in the DS-AWD treatment peak concentrations prior to the second fertilization were observed at 25 cm on June 3rd, reaching 18.5 ± 8.3 µg N₂O-N L⁻¹.

As with dissolved N₂O, pore air N₂O concentrations were highly variable between treatments and between sampling days and are again presented on a log₁₀ scale (Fig. 2) and non-transformed scale (Fig. S4). In both WS treatments, the highest concentrations were observed on the first day of measurement, May 20th, reaching 2903.3 ± 1103.6 and 1321 ± 998.0 µg N₂O-N L⁻¹ at 5 cm in the WS-FLD and WS-AWD, respectively. Elevated concentrations of N₂O_{poreair} were also observed in the DS-AWD on the first day of measurement but were 70.1 µg N₂O-N L⁻¹ at 5 cm (roughly 40x lower than in WS-FLD on this date). Maximum concentrations in the DS-AWD treatment were observed two days after the second fertilizer application, reaching 1902.2 µg N₂O-N L⁻¹; in contrast no change was observed in the WS treatments following this fertilizer application. In all treatments the majority of N₂O_{poreair} concentrations were orders of magnitude lower than these peaks. There was a tendency of lower N₂O_{poreair} concentrations in the DS-AWD treatment relative to the WS treatments; this pattern was most evident at 5 cm (Fig. 2). However, treatment differences in N₂O_{poreair} were not significant ($p=0.08$, Table S3) and there was a significant date x treatment interaction.



3.1.2 Relation of N_2O fluxes and concentrations with soil environment, substrates and N_2O isotopocules

We evaluated the correlation of $\text{N}_2\text{O}_{\text{emitted}}$ with Eh, WFPS, NO_3^- , NH_4^+ , dissolved and pore air N_2O concentrations and N_2O isotopocule ratios at 5 cm (Table 3). Among these variables, N_2O emissions in the WS treatments were negatively correlated with pore water NH_4^+ and DOC in the WS-AWD treatment. In the DS-AWD treatment, emissions positively correlated with $\text{N}_2\text{O}_{\text{poreair}}$, WFPS, and NO_3^- and negatively with N_2O isotopocule signatures. Examining the isotopocule signatures of $\text{N}_2\text{O}_{\text{emitted}}$, we observed that $\text{N}_2\text{O}_{\text{emitted}}$ was negatively correlated with $\delta^{18}\text{O}-\text{N}_2\text{O}_{\text{emitted}}$ in all treatments, negatively with $\delta^{15}\text{N}-\text{N}_2\text{O}_{\text{emitted}}$ in the DS-AWD treatment and negatively with $\text{SP}-\text{N}_2\text{O}_{\text{emitted}}$ in the WS-FLD and DS-AWD. Interestingly, a positive correlation between $\text{N}_2\text{O}_{\text{emitted}}$ and $\text{SP}-\text{N}_2\text{O}_{\text{emitted}}$ was observed in the WS-AWD treatment. Relative to the DS-AWD, the WS treatments had fewer significant correlations between N_2O isotopocules, soil environment or pore air N_2O isotopocule signatures. DOC was positively correlated with $\delta^{15}\text{N}-\text{N}_2\text{O}_{\text{emitted}}$ in the WS-AWD and with $\delta^{18}\text{O}-\text{N}_2\text{O}_{\text{emitted}}$ in the WS-FLD. $\text{SP}-\text{N}_2\text{O}_{\text{emitted}}$ was positively correlated to Eh and negatively to WFPS in the WS-AWD treatment. In comparison, in the DS-AWD treatment, N_2O isotopocules signatures of $\text{N}_2\text{O}_{\text{emitted}}$ were positively correlated to that of $\text{N}_2\text{O}_{\text{poreair}}$ for all three isotopocules. Furthermore, N_2O isotopocule signatures in the DS-AWD treatment were negatively correlated with $\text{N}_2\text{O}_{\text{poreair}}$ concentrations, WFPS, NO_3^- ($\delta^{15}\text{N}-\text{N}_2\text{O}_{\text{emitted}}$ only) and $\text{N}_2\text{O}_{\text{dissolved}}$ ($\delta^{18}\text{O}-\text{N}_2\text{O}_{\text{emitted}}$ and $\text{SP}-\text{N}_2\text{O}_{\text{emitted}}$ only). It should be noted that $\text{N}_2\text{O}_{\text{dissolved}}$ in the DS-AWD treatment was not measurable at the 5 cm depth on 10 of the 16 sampling dates due to low soil moisture and low pore water volumes.

3.2 Spatiotemporal patterns of N_2O isotopocules

3.2.1 $\delta^{15}\text{N}-\text{N}_2\text{O}$

The $\delta^{15}\text{N}$ signatures of $\text{N}_2\text{O}_{\text{emitted}}$ showed high temporal variation across all treatments, while $\delta^{15}\text{N}-\text{N}_2\text{O}_{\text{poreair}}$ signatures changed less between sample dates and more discernable patterns across time could be seen (Fig. 3). A consistent temporal pattern of higher $\text{N}_2\text{O}_{\text{poreair}}$ concentrations and $\text{N}_2\text{O}_{\text{emitted}}$ fluxes in association with lower $\delta^{15}\text{N}$ signatures was observed in the DS-AWD treatment. In the WS treatments, high $\text{N}_2\text{O}_{\text{emitted}}$ fluxes were also associated with lower $\delta^{15}\text{N}$ signatures. $\text{N}_2\text{O}_{\text{poreair}}$ at 5cm in the WS-AWD treatment tended to be higher in concentration and lower in $\delta^{15}\text{N}$ relative to other depths, however, in general a consistent relationship between concentration and $\delta^{15}\text{N}$ signatures was less evident in the two WS treatments. On average, the $\delta^{15}\text{N}$ signature of $\text{N}_2\text{O}_{\text{emitted}}$ was lower relative to $\text{N}_2\text{O}_{\text{poreair}}$ in the DS-AWD treatment. In contrast, in the WS treatments $\text{N}_2\text{O}_{\text{emitted}}$ was depleted in ^{15}N relative to $\text{N}_2\text{O}_{\text{poreair}}$ at all depths only immediately before and after the second fertilization. In these treatments, $\delta^{15}\text{N}-\text{N}_2\text{O}_{\text{poreair}}$ was generally lower at 5 cm relative the other depths but tended to increase and reach similar values as the other depths over the experimental period. As a result, $\text{N}_2\text{O}_{\text{emitted}}$ was often enriched in ^{15}N relative to $\text{N}_2\text{O}_{\text{poreair}}$ at 5 cm in these treatments, particularly in the WS-AWD treatment.



3.2.2 $\delta^{18}\text{O}\text{-N}_2\text{O}$

As with $\delta^{15}\text{N}$, $\delta^{18}\text{O}$ signatures spanned a large range, particularly in the emitted N_2O (Fig. 3). $\delta^{18}\text{O}\text{-N}_2\text{O}_{\text{poreair}}$ in the DS-AWD followed a temporal pattern similar to $\delta^{15}\text{N}$ signatures and similarly, $\delta^{18}\text{O}$ signatures were generally lower in $\text{N}_2\text{O}_{\text{emitted}}$ relative to $\text{N}_2\text{O}_{\text{poreair}}$. The highest $\delta^{18}\text{O}\text{-N}_2\text{O}_{\text{poreair}}$ was seen in the DS-AWD treatment at moderate $\text{N}_2\text{O}_{\text{poreair}}$ concentrations where $\delta^{18}\text{O}$ signatures were higher than other concentrations in the DS-AWD or any concentration in the WS treatments. These samples were also nearly always taken from 12.5 or 25 cm. In all treatments, lower $\delta^{18}\text{O}$ signatures were observed in $\text{N}_2\text{O}_{\text{poreair}}$ and $\text{N}_2\text{O}_{\text{emitted}}$ on the first day of sampling, global mean of 35.1 ± 1.1 and $29.6 \pm 1.7\text{‰}$ relative to 46.9 ± 0.4 and $43.9 \pm 1.7\text{‰}$, respectively. Otherwise, no distinct pattern with depth, time, or concentration was observed in the WS treatments.

3.2.3 SP- N_2O

The SP of $\text{N}_2\text{O}_{\text{emitted}}$ ranged from 4.5 ± 0.4 to $25.6 \pm 8.1\text{‰}$, from 2.9 ± 1.0 to 37.2‰ (un-replicated) and from 5.8 ± 0.6 to $40.6 \pm 12.4\text{‰}$, in the DS-AWD, WS-AWD, and WS-FLD treatments, respectively (Fig. 3). In contrast to $\delta^{15}\text{N}$ and $\delta^{18}\text{O}$ signatures, the SP- $\text{N}_2\text{O}_{\text{poreair}}$ tended to increase with time, but only in the WS treatments. As with $\delta^{15}\text{N}\text{-N}_2\text{O}$ and $\delta^{18}\text{O}\text{-N}_2\text{O}$, moderate and lower concentration $\text{N}_2\text{O}_{\text{poreair}}$ samples showed higher SP values relative to higher concentration $\text{N}_2\text{O}_{\text{poreair}}$ samples. For example, two days after the second fertilizer application (June 23rd), SP values decreased in conjunction with increased $\text{N}_2\text{O}_{\text{poreair}}$ concentrations in the DS-AWD treatment. On this date mean SP values at 5 cm demonstrated the largest treatment differences with values of: 0.7 ± 4.5 , 27.6 ± 2.1 , and $39.9 \pm 2.7\text{‰}$ in the DS-AWD, WS-AWD, and WS-FLD treatments, respectively. On this date, the pattern between the treatments was consistent throughout the three depths.

3.2.4 Relationships between N_2O isotopocules

Considering all depths and emitted data together, $\delta^{18}\text{O}\text{-N}_2\text{O}$ signatures significantly and positively correlated with $\delta^{15}\text{N}\text{-N}_2\text{O}$ and SP across all treatments. The slope of $\delta^{18}\text{O}\text{-N}_2\text{O}$ vs. $\delta^{15}\text{N}\text{-N}_2\text{O}$ was 0.67, 0.28, and 0.52 (Fig. S5) and 0.67, 0.54 and 0.31 for SP vs. $\delta^{18}\text{O}\text{-N}_2\text{O}$ in the DS-AWD, WS-AWD, and WS-FLD treatments, respectively (Fig. 4a). There was no correlation between SP and $\delta^{15}\text{N}\text{-N}_2\text{O}$ in the two WS treatments, but a positive correlation for the DS-AWD was found, with a slope of 0.62 (Fig. 4b). Examining these relationships by depth, we saw the strongest relationship and highest slope in the $\text{N}_2\text{O}_{\text{emitted}}$ and at 25 cm for $\delta^{18}\text{O}\text{-N}_2\text{O}$ vs $\delta^{15}\text{N}\text{-N}_2\text{O}$ (Fig. S5). While the SP vs $\delta^{18}\text{O}\text{-N}_2\text{O}$ showed no correlation among the surface fluxes in the WS treatments, the two isotopocules were positively correlated in $\text{N}_2\text{O}_{\text{poreair}}$ at all depths and treatments (Fig. S6). A contrasting relationship between SP and $\delta^{15}\text{N}\text{-N}_2\text{O}$ was observed for the WS-FLD treatment in the $\text{N}_2\text{O}_{\text{emitted}}$ and $\text{N}_2\text{O}_{\text{poreair}}$ where the two isotopocules were negatively correlated in $\text{N}_2\text{O}_{\text{emitted}}$ and positively in $\text{N}_2\text{O}_{\text{poreair}}$ (Fig. S7).



3.3 NO_3^- and NH_4^+ concentrations and isotope signatures

3.3.1 Spatiotemporal trend in NO_3^- and NH_4^+ concentration and $\delta^{15}\text{N}$ and $\delta^{18}\text{O}$ signatures

In all treatments, pore water NH_4^+ concentrations were highest at 5 cm relative to the other depths (Fig. 2). In the DS-AWD treatment concentrations were almost null prior to the second fertilization, remaining below $0.85 \text{ mg NH}_4^+\text{-N L}^{-1}$ across all depths. Following this fertilization, concentrations increased at all depths, most notably at 5 cm. An opposing pattern was observed in the WS treatments where NH_4^+ was nearly always significantly higher than in DS-AWD for each corresponding depth leading up to the second fertilization, but dropped to near zero following the fertilization. Nitrate concentrations were exclusively less than $1.5 \text{ mg NO}_3\text{-N L}^{-1}$ in both WS treatments throughout the experimental period. In sharp contrast, NO_3^- concentrations in the DS-AWD were at times more than 75 times higher than in WS treatments, peaking on June 1st at $113.6 \pm 22.4 \text{ mg NO}_3\text{-N L}^{-1}$. Following this spike, concentrations steadily declined and dropped to null following the second fertilization.

3.3.2 $\delta^{15}\text{N}\text{-NO}_3^-$, $\delta^{15}\text{N}\text{-NH}_4^+$ and isotope enrichment factors: $\epsilon^{15}\text{N}_{\text{N}_2\text{O}/\text{NO}_3}$ and $\epsilon^{15}\text{N}_{\text{N}_2\text{O}/\text{NH}_4}$

Concentrations of NO_3^- or NH_4^+ were often too low for isotope measurements. Hence, we could only obtain sufficient replication for statistical analysis across depths and treatments on five days for NO_3^- (May 24th, 27th, June 1st, 14th, 23rd) and two days for NH_4^+ (May 24th and June 23rd) (Fig. S9). Daily mean $\delta^{15}\text{N}\text{-NO}_3^-$ ranged from -4.3 to 28.3‰ across all treatments and depths. In the DS-AWD treatment a consistent depth pattern was observed with ^{15}N enrichment of NO_3^- at $25 \text{ cm} > 12.5 \text{ cm} = 5 \text{ cm}$. $\delta^{15}\text{N}\text{-NO}_3^-$ signatures increased with time at 5 cm, rising from $-4.3 \pm 1.5\text{‰}$ to $22.0 \pm 4.9\text{‰}$. Significant treatment and depth differences were observed on May 24th, 27th and June 1st, but no differences were observed on later dates, June 14th or 23rd. Following the second fertilizer application, $\delta^{15}\text{N}\text{-NO}_3^-$ signatures in the DS-AWD treatment rose by approximately 10‰ at all depths. Daily mean $\delta^{15}\text{N}\text{-NH}_4^+$ ranged from -6‰ to 15.2‰ (Fig. S9). Averaging across the experimental period and depths, mean $\delta^{15}\text{N}$ signatures of NO_3^- and NH_4^+ were similar, 8.4 and 7.0‰ , respectively (Table S5). There was no evident temporal or depth trend in $\delta^{15}\text{N}\text{-NH}_4^+$ in any of the treatments. The only significant difference was lower $\delta^{15}\text{N}\text{-NH}_4^+$ in the DS-AWD on June 23rd. $\delta^{15}\text{N}\text{-NO}_3^-$ values positively correlated to $\text{N}_2\text{O}_{\text{poreair}}$ concentrations in the DS-AWD and WS-FLD treatments and were negatively correlated to NO_3^- concentrations and to $\delta^{15}\text{N}\text{-NH}_4^+$ in the DS-AWD treatment (Table 4). $\delta^{15}\text{N}\text{-NH}_4^+$ was negatively correlated to $\text{N}_2\text{O}_{\text{poreair}}$ concentrations and NH_4^+ concentrations and positively to $\delta^{15}\text{N}\text{-N}_2\text{O}_{\text{poreair}}$ in the DS-AWD treatment.

Largely reflecting the depth pattern of $\delta^{15}\text{N}\text{-NO}_3^-$ in the DS-AWD, the calculated $\epsilon^{15}\text{N}_{\text{N}_2\text{O}/\text{NO}_3}$ tended to be highest at 5 cm, mean $-7.2 \pm 2.7\text{‰}$, while mean values at 12.5 and 25 cm were slightly lower, -9.5 ± 2.0 and $-16.0 \pm 2.1\text{‰}$, respectively (Fig. S9). At 5 cm $\epsilon^{15}\text{N}_{\text{N}_2\text{O}/\text{NO}_3}$ values in the DS-AWD were significantly higher than in the WS treatments; at 12.5cm they tended to be higher as well but the difference was not significant. Two days after the second fertilizer application, the $\epsilon^{15}\text{N}_{\text{N}_2\text{O}/\text{NO}_3}$ in the DS-AWD markedly decreased at all depths to a treatment mean of $-23.6 \pm 2.6\text{‰}$. In comparison, WS treatment $\epsilon^{15}\text{N}_{\text{N}_2\text{O}/\text{NO}_3}$



values rose one (WS-FLD) or two (WS-AWD) days following the fertilization. In the WS-FLD, the increase in $\epsilon^{15}\text{N}_{\text{N}_2\text{O}/\text{NO}_3}$ values lasted only one day; unfortunately low NO_3^- concentrations precluded $\delta^{15}\text{N}-\text{NO}_3^-$ analysis on many dates making temporal patterns difficult to observe. Mean depth by treatment isotope effects calculated relative to $\delta^{15}\text{N}-\text{NH}_4^+$ ($\epsilon^{15}\text{N}_{\text{N}_2\text{O}/\text{NH}_4}$) were $-12.7 \pm 3.2\text{‰}$, $-24.5 \pm 2.6\text{‰}$ and $-20.6 \pm 2.2\text{‰}$ at 5 cm; $-9.9 \pm 4.0\text{‰}$, $-12.8 \pm 2.8\text{‰}$ and $-15.9 \pm 1.9\text{‰}$ at 12.5 cm; $-17.0 \pm 5.9\text{‰}$, $-6.4 \pm 1.7\text{‰}$ and $-5.8 \pm 2.7\text{‰}$ at 25 cm for DS-AWD, WD-AWD and WD-FLD, respectively. Data for $\epsilon^{15}\text{N}_{\text{N}_2\text{O}/\text{NH}_4}$ was scarce in the DS-AWD treatment due to low NH_4^+ concentrations, in the WS treatments $\epsilon^{15}\text{N}_{\text{N}_2\text{O}/\text{NH}_4}$ increased with depth, but these differences were not significant.

$\delta^{18}\text{O}-\text{NO}_3^-$ was significantly depleted in the DS-AWD treatment relative to both WS treatments (Fig. S9). Prior to the second fertilization, values were remarkably consistent in the DS-AWD at all depths, ranging from 0.1 to 7.5‰. Two days after this fertilizer application, $\delta^{18}\text{O}-\text{NO}_3^-$ rose to a mean of 7.6‰ across depths. In comparison the $\delta^{18}\text{O}-\text{NO}_3^-$ of both WS treatments was more variable between sampling dates, fluctuating between 12.2 to 38.8 and 10.4 to 32.7‰ leading up the second fertilization in the WS-AWD and WS-FLD, respectively. Two days after the second fertilizer application values rose to a mean of 23.7 and 27.4‰ across depths in the WS-AWD and WS-FLD, respectively. We calculated the net isotope effect for $\delta^{18}\text{O}$ relative to water ($\epsilon^{18}\text{O}_{\text{N}_2\text{O}/\text{H}_2\text{O}}$). The $\epsilon^{18}\text{O}_{\text{N}_2\text{O}/\text{H}_2\text{O}}$ in all treatments and depths tended to rise over the course of the measurement period, with the most consistent rise observed at 5 cm. Here values rose from a global mean of $43.8 \pm 1.0\text{‰}$ on May 20th to $58.5 \pm 1.0\text{‰}$ on June 30th. There was a pattern of higher $\epsilon^{18}\text{O}_{\text{N}_2\text{O}/\text{H}_2\text{O}}$ in the DS-AWD treatment relative to the two WS treatments. A drop in $\epsilon^{18}\text{O}_{\text{N}_2\text{O}/\text{H}_2\text{O}}$ of $\sim 10\text{‰}$ was observed in all depths on June 23rd, two days after the second fertilization with urea, in the DS-AWD only.

3.4 SP x $\delta^{18}\text{O}-\text{N}_2\text{O}$ two endmember mixing model to estimate N_2O reduction, source contributions, and N_2O reduction

To further quantitatively interpret our isotopocule data, we employed a graphical two end-member mixing model (Lewicka-Szczebak *et al.*, 2017), based on the relationship between SP and $\delta^{18}\text{O}-\text{N}_2\text{O}$ (Fig. 1 and 4). Data was modeled for open and closed fraction dynamics under two scenarios. In sc1 reduction of N_2O from the denitrification/nitrifier-denitrification endmember pool occurs prior to mixing with nitrification/fungal denitrification derived N_2O ; in sc2, mixing of N_2O from both endmember pools occurs before reduction. For sc2 our model yielded implausible results for the contribution of denitrification/nitrifier-denitrification to N_2O emissions in about 90% and 20% of observations under open and closed system dynamics, respectively (Table S2). The poorer outcomes from sc2 in the open system indicate that the assumptions underlying this scenario are likely false in open systems or vice versa. In order to have comparable data between open and closed systems we discuss only results coming from sc1 simulations.

Temporal trends in the gross rates of $r\text{N}_2\text{O}$ (extent of N_2O reduction) predicted by open and closed system N_2O fractionation were nearly identical (Fig. 5b). Gross $r\text{N}_2\text{O}$ was estimated to be higher (i.e. lower N_2O reduction) under closed system fractionation dynamics. In reality, it can be assumed that neither perfect open or closed systems exist in nature and processes



likely reflect a mixture of these dynamics. The use of one or the other case may bias results, therefore we chose to take the mean of the two systems to estimate N_2O reduction, nitrification/fungal denitrification and denitrification/nitrifier-denitrification derived N_2O emissions (Decock and Six, 2013b; Wu *et al.*, 2016). Due to a disproportionate number of missing values at 25 cm in the two WS treatments, we chose not to include data from this depth in our analysis and discussion.

5 Therefore, further values refer to the mean of open and closed systems and $\text{N}_2\text{O}_{\text{emitted}}$ or $\text{N}_2\text{O}_{\text{poreair}}$ at 5 cm and 12.5 cm unless explicitly stated otherwise. Gross $r\text{N}_2\text{O}$ fractions tended to be higher in $\text{N}_2\text{O}_{\text{emitted}}$ (treatment means 0.14 to 0.19) relative to the subsurface (treatment means 0.06 to 0.15). While water management treatment had a significant effect on process contributions to $\text{N}_2\text{O}_{\text{emitted}}$ and $\text{N}_2\text{O}_{\text{poreair}}$ (Table 5), significant interactions with depth and date were observed. Gross $r\text{N}_2\text{O}$ fractions in $\text{N}_2\text{O}_{\text{poreair}}$ were significantly lower in the DS-AWD relative to the WS-FLD on six of 15 days, with the WS-AWD

10 falling in between. In the $\text{N}_2\text{O}_{\text{emitted}}$, the opposite pattern was mostly observed with gross $r\text{N}_2\text{O}$ fractions often being higher in the DS-AWD than one or the other WS treatments, significantly so on four of 15 days. Aggregated across depths, the contribution of denitrification/nitrifier-denitrification to $\text{N}_2\text{O}_{\text{poreair}}$ were higher in the DS-AWD relative to one or both WS treatments on four dates and lower on three dates (Fig. 5a). The mean contribution of denitrification/nitrifier-denitrification to $\text{N}_2\text{O}_{\text{emitted}}$ ranged from 43 to 49% in all treatments (Fig. 6). Denitrification/nitrifier-denitrification contributions to $\text{N}_2\text{O}_{\text{emitted}}$

15 were higher in the DS-AWD relative to the WS treatments on June 9th and 23rd and relative to WS-AWD only they were also higher on June 28th and lower on June 21st.

4 Discussion

4.1 Patterns of $\text{N}_2\text{O}_{\text{emitted}}$, $\text{N}_2\text{O}_{\text{poreair}}$, N_2O isotopocule ratios and net isotope effects

In accordance with results from past studies (Cai *et al.*, 1997; Miniotti *et al.*, 2016; Peyron *et al.*, 2016) and in line with our

20 hypothesis, we observed higher N_2O emissions on most days in the DS-AWD relative to the two WS treatments (Fig. 2). A belated divergence in water management between the WS-FLD and WS-AWD (Table 1), in addition to a relatively wet early summer, likely contributed to similar observed soil environmental conditions and N substrates among these two treatments. Therefore, given the similarities in soil conditions, it is not surprising that N_2O fluxes and isotopocule differences between these two treatments were generally fewer than expected.

25

Mean daily $\delta^{15}\text{N}$, $\delta^{18}\text{O}$ and SP values of $\text{N}_2\text{O}_{\text{emitted}}$ and $\text{N}_2\text{O}_{\text{poreair}}$ per depth and treatment ranged from -27.9 to 12.3‰, 30.9 to 63.0‰ and -14.0 to 53.2‰, respectively (Fig. 3). These values are similar in magnitude to those observed by Yano *et al.*, (2014) in the early growing season of rice, where ranges of -24 to 6‰, 24 to 66‰ and 4 to 25‰ were reported. Our values are also similar in magnitude to those observed in other field studies which have included depth sampling (Koehler *et al.*, 2012;

30 Zou *et al.*, 2014). Relative to these two studies we observed higher $\delta^{15}\text{N}$ - N_2O and both higher and lower SP ratios. This was likely due to a higher sampling frequency, which covered more variable soil environments and generally higher soil moisture in our study than in the others. For example, it has been shown that organic matter decomposition and DOC availability in



rice systems can decline with the introduction of wet-dry cycles or dry seeding (Yao *et al.*, 2011; Said-Pullicino *et al.*, 2016); thus it is likely that conditions promoting complete denitrification declined in the AWD treatments. While, saturated conditions promoting complete denitrification may have a strong impact on isotope signatures. Working in a denitrifying aquifer, Well *et al.* (2012) observed very large ranges in $\delta^{15}\text{N}$ and SP ratios, varying from -55.4 to 89.4‰ and 1.8 to 97.9‰, respectively.

The calculated $\epsilon^{15}\text{N}_{\text{N}_2\text{O}/\text{NO}_3}$ (net isotope effect) in the DS-AWD treatment, with depth means of -7.2 to -16.0‰, was consistently much higher (i.e. less strong fractionation) than literature values reported for denitrification of NO_3^- , mean: $-42.9 \pm 6.3\%$ (Denk *et al.*, 2017)(Fig. S9). At 5 cm in the two WS treatments, the mean $\epsilon^{15}\text{N}_{\text{N}_2\text{O}/\text{NO}_3}$ was lower than in the DS-AWD (-23.2 and -21.5 in the WS-AWD and WS-FLD, respectively), but still nearly 20‰ higher than literature values. In a rice system, Yano *et al.* (2014) observed an $\epsilon^{15}\text{N}_{\text{N}_2\text{O}/\text{NO}_3}$ of -6.7‰, thus very well within the range of our calculated $\epsilon^{15}\text{N}_{\text{N}_2\text{O}/\text{NO}_3}$. Similarly, the global mean of our $\epsilon^{15}\text{N}_{\text{N}_2\text{O}/\text{NH}_4}$ values was -14.8‰, thus on average much higher than those reported in the literature for nitrification, -46.9‰ (Sutka *et al.*, 2006) or $-56.6 \pm 7.3\%$ (Denk *et al.*, 2017). For both isotope effects, similar scenarios may explain our high observed $\epsilon^{15}\text{N}_x$ (i.e. low fractionation). Namely, i) non-steady state reactions, for example rapid refreshing of the NO_3^- and NH_4^+ pools or near complete substrate consumption or ii) significant reduction of N_2O serving to increase $\delta^{15}\text{N}\text{-N}_2\text{O}$ values and thereby reduce the net isotope effect.

Considering the moist conditions and high reduction rates, it seems most likely that strong N_2O reduction was the largest contributor to our high net isotope effects. To check this, we estimated *initial* $\delta^{15}\text{N}\text{-N}_2\text{O}$ values before N_2O reduction using our modeled N_2O reduction fraction ($r_{\text{N}_2\text{O}}$), measured $\delta^{15}\text{N}\text{-N}_2\text{O}$ values and a ^{15}N isotope effect during reduction of -6.6‰ (Denk *et al.*, 2017) in the Rayleigh equation. We could then estimate amended $\epsilon^{15}\text{N}_{\text{N}_2\text{O}/\text{NO}_3}$ values if N_2O reduction effects were accounted for, from the difference between our *initial* $\delta^{15}\text{N}\text{-N}_2\text{O}$ estimates and $\delta^{15}\text{N}\text{-NO}_3^-$. These calculations yielded a $\epsilon^{15}\text{N}_{\text{N}_2\text{O}/\text{NO}_3}$ from -25.0 to -36.5‰, -32.6 to -42.3‰ and -29.0 to -51.1‰ in the DS-AWD, WS-AWD and WS-FLD across depths (Table S6). These amended $\epsilon^{15}\text{N}_{\text{N}_2\text{O}/\text{NO}_3}$ values do decrease and especially for the WS treatments, come relatively close to literature values for $\epsilon^{15}\text{N}_{\text{N}_2\text{O}/\text{NO}_3}$ values during denitrification. Thus, significant N_2O reduction can likely explain much of the high $\epsilon^{15}\text{N}_{\text{N}_2\text{O}/\text{NO}_3}$ values observed, particularly in the WS treatments. Yet other factors were also likely at play to some degree. For example, in the DS-AWD, where we observed evidence of significant nitrification, it is quite possible to envision isolated enrichment of NO_3^- in anaerobic microsites where N_2O is produced, while the bulk soil NO_3^- pool remained less enriched. It is also true that we could not always measure $\delta^{15}\text{N}$ values of NO_3^- or NH_4^+ because the concentrations were too low, thus we could not calculate isotope effects. This highlights a persistent dilemma, which is true for all isotopocules, that we cannot accurately measure isotope values at very low concentrations. Hence, *in situ* measurements such as these will always be biased toward higher concentration scenarios where perhaps the strongest and most interesting effects of substrate enrichment are missed.



4.2 Source partitioning N₂O production

The use of any one isotope signature alone is confounded by overlap in the isotope effects between processes, unknown and possibly rapidly changing substrate δ values and the unknown contribution of N₂O reduction effects. To overcome these drawbacks, graphical interpretations of dual N₂O isotopocules have been used in field studies to interpret datasets similar to ours (Koehler *et al.*, 2012; Well *et al.*, 2012). For a more quantitative assessment of source-partitioning, mixing models using a dual isotope approach can be used (Koba *et al.*, 2009; Toyoda *et al.*, 2011; Yano *et al.*, 2014; Zou *et al.*, 2014; Lewicka-Szczebak *et al.*, 2017). In the subsequent analysis we employ both approaches using our samples values plotted in SP x $\delta^{18}\text{O}$ and SP x $\delta^{15}\text{N}$ space (Fig. 4 and Figs.S10-S12).

In both SP x $\delta^{18}\text{O}$ and SP x $\delta^{15}\text{N}$ plots our sample values mostly fell between the mixing and reduction lines predicted by either isotopocule relationship (Fig. 4) and somewhat surprisingly showed a stronger trajectory towards N₂O reduction in the DS-AWD treatment relative to the WS treatments. In the DS-AWD and to a lesser extent in the WS-AWD treatment, high pore air N₂O concentrations were associated with denitrification or nitrifier-denitrification, while mid-range concentrations were associated with a higher degree of N₂O reduction and the lowest concentrations fell neatly in between. Similarly, in the WS-FLD treatment, denitrification or nitrifier-denitrification associated samples almost exclusively coincided with high N₂O_{poreair}. Most likely the moderate N₂O_{poreair} concentrations derived from N₂O reduction following high denitrification/nitrifier-denitrification production. This analysis is supported by data showing a trend of enrichment over the course of the measurement period (Fig. S10) and high WFPS values associated with the most enriched N₂O_{poreair} in the DS-AWD (Fig. S12). All treatments showed an enrichment of SP with time (Fig. S10), but interestingly only in the DS-AWD did $\delta^{18}\text{O}$ and $\delta^{15}\text{N}$ -N₂O enrich over the course of the experiment. This may reflect an increase over time in $\delta^{15}\text{N}$ and $\delta^{18}\text{O}$ of NO₃⁻, which was observed in the DS-AWD treatment, albeit not strongly (Fig. S9), yet one could expect a stronger enrichment of $\delta^{15}\text{N}$ and $\delta^{18}\text{O}$ -NO₃⁻ in denitrifying microsites.

We observed a scattering of high to moderate concentration N₂O_{poreair} values in the WS treatments that corresponded to higher SP values relative to $\delta^{18}\text{O}$ or $\delta^{15}\text{N}$ than would be expected by reduction enrichment (Fig. 4). We postulate that these values could be explained by greater contributions from abiotic hydroxylamine decomposition (SP ~ 34-35‰, Heil *et al.* (2014)) or fungal denitrification (SP ~ 35‰, Rohe *et al.* (2014)). Zhou *et al.* (2001) showed that fungal denitrification requires minimal oxygen to proceed, similarly Seo and DeLaune (2010) found that fungal denitrification dominated relative to bacterial denitrification at modest reducing conditions to weakly oxidizing conditions (Eh >250 mV). Indeed, there is some evidence that these high scattered SP values corresponded to more moderate WFPS (70-90%) in the WS-FLD treatment (Fig. S12). Abiotic hydroxylamine decomposition requires nitrification for the production of NH₂OH, and iron or manganese (hydr)oxides as electron acceptors to proceed (Bremner *et al.*, 1980). These species can co-occur in the rhizosphere of a flooded rice soil, where O₂ is transported to the immediate root zone by the aerenchyma, for example, tightly coupled



nitrification-denitrification in the rhizosphere of rice plants has been shown before (Arth and Frenzel, 2000) as has coupling of nitrogen – iron transformations (Ratering and Schnell, 2000).

It is necessary to contextualize N_2O isotopocule data with our measured substrate concentrations and soil environmental data.

5 Based on our observations of low NH_4^+ concentrations, high NO_3^- concentrations, an Eh over 400 mV and WFPS often below 60% (5 cm) or below 85% (12.5 and 25 cm) in the DS-AWD treatment, we can safely deduce that extensive nitrification of either basal urea fertilizer or of indigenous soil N occurred in this treatment (Fig. 2). Furthermore, the $\delta^{18}\text{O}-\text{NO}_3^-$ in the DS-AWD treatment ranged from 0.1 to 14.8 (Fig. 7), thus falling in the range attributed to NO_3^- produced from nitrification (Kendall and McDonnell, 2012). Additionally, we observed that both $\delta^{15}\text{N}-\text{NO}_3^-$ and $\delta^{15}\text{N}-\text{NH}_4^+$ were negatively correlated to
 10 substrate concentrations in the DS-AWD treatment, indicative of active consumption of both N substrates (Table 4). In the DS-AWD, there also was a positive correlation between $\delta^{15}\text{N}-\text{NO}_3^-$ and $\text{N}_2\text{O}_{\text{poreair}}$ but a negative correlation between $\delta^{15}\text{N}-\text{NH}_4^+$ and $\text{N}_2\text{O}_{\text{poreair}}$. The former likely indicates N_2O production via denitrification and subsequent enrichment of the NO_3^- pool. The latter is more difficult to interpret, but we attributed this to higher emissions associated with fresh inputs of NH_4^+ (from urea or mineralization) which should have a $\delta^{15}\text{N}$ value around 0‰. Together this data shows that coupled nitrification-
 15 denitrification was responsible for the majority of N_2O emissions. Similar results were also reported by Dong *et al.* (2012) for an AWD system. The separation of isotopocule signatures by date, N_2O concentration and WFPS suggests that NO_3^- produced early in the growing season was progressively denitrified and reduced over the course of the sampling period. Similarly, N_2O produced early in the growing season may have been progressively reduced.

4.3 Inferring the extent of N_2O reduction

20 It has been suggested that the slope of $\text{SP}/\delta^{18}\text{O}$, $\text{SP}/\delta^{15}\text{N}$ and $\delta^{18}\text{O}/\delta^{15}\text{N}$ or their isotope effects can be used to estimate the extent of N_2O reduction (Ostrom *et al.*, 2007; Jinuntuya-Nortman *et al.*, 2008; Well and Flessa, 2009; Lewicka-Szczebak *et al.*, 2017). However, many studies deriving these relationships have taken place under controlled conditions when N_2O supply was often limited. Therefore fractionation followed closed system dynamics would result in larger fractionation effects on the residual substrate than under open system dynamics. The positive and significant relationship between all isotopocules and
 25 across all depths in the DS-AWD treatment suggests an influence of reduction at all depths. In contrast, in the WS treatments we observed no relationship between SP and $\delta^{18}\text{O}$ within $\text{N}_2\text{O}_{\text{emitted}}$ (Fig. S7) and only a weak relationship between SP and $\delta^{15}\text{N}$ at 25 cm in the WS-AWD, and even a negative relationship between SP and $\delta^{15}\text{N}$ in the WS-FLD $\text{N}_2\text{O}_{\text{emitted}}$ (Fig. S8). The range of observed $\delta^{18}\text{O}/\delta^{15}\text{N}$ slopes, 0.21 to 0.90, (Fig. S5) were substantially lower than those observed in many N_2O reduction studies (1.94 to 2.6; Jinuntuya-Nortman *et al.* (2008); Ostrom *et al.* (2007); Well and Flessa (2009); Lewicka-Szczebak *et al.* (2017)), but closer to the 0.45 slope observed by Yano *et al.* (2014) in an *in situ* rice field study. When a
 30 significant relationship was observed, overall or $\text{N}_2\text{O}_{\text{poreair}}$ $\text{SP}/\delta^{15}\text{N}$ slopes ranged from 0.49 to 0.83 (Fig. 4b). These slopes are either close to those of other field studies, 0.48 to 0.52 (Yano *et al.*, 2014; Wolf *et al.*, 2015) or intermediary between field studies and controlled N_2O reduction studies, 0.59 to 1.01 (Well and Flessa (2009); Lewicka-Szczebak *et al.* (2017)). From



controlled N_2O reduction studies, a $\text{SP}/\delta^{18}\text{O}$ slope between 0.2 to 0.4 has been observed (Jinuntuya-Nortman *et al.*, 2008; Well and Flessa, 2009), thus in this case the $\text{N}_2\text{O}_{\text{poreair}}$ slopes observed in our study were substantially higher (Fig. 4a and Fig. S7). The lower overall SP and $\delta^{18}\text{O}$ slope in the WS treatments was due to inclusion of the $\text{N}_2\text{O}_{\text{emitted}}$ values, which individually showed no relationship in these treatments.

5

A deviation in slopes compared to those observed in controlled N_2O reduction studies likely points to a growing influence of open system dynamics where substrates are continuously refreshed. It has been demonstrated that when mixing processes dominate over reduction processes, the $\text{SP}/\delta^{18}\text{O}$ slope rises (Lewicka-Szczebak *et al.*, 2017). It is also plausible that high rates of oxygen exchange during denitrification served to partially mask an increase in $\delta^{18}\text{O}-\text{N}_2\text{O}$ values, resulting in the higher observed $\text{SP}/\delta^{18}\text{O}$ slopes or lower $\delta^{18}\text{O}/\delta^{15}\text{N}$ slopes. To estimate the extent of oxygen exchange with denitrification precursors (NO_x) we plotted $\delta^{18}\text{O}-\text{N}_2\text{O}/\delta^{18}\text{O}-\text{NO}_3^-$ by $\delta^{18}\text{O}-\text{H}_2\text{O}/\delta^{18}\text{O}-\text{NO}_3^-$ following (Snider *et al.*, 2009). The slope of this relationship ranged from 0.7 to 2.1 (data not shown). Thus we assume oxygen exchange was effectively 100% across treatments during denitrification. In summary, the observed positive relationships between the isotopocule pairs is indicative of an influential role of N_2O reduction in the DS-AWD treatment. This is less clear in the WS treatments where relationships were more erratic, suggesting a stronger influence of changing nitrification and denitrification process rates or changing $\delta^{15}\text{N}$ of N substrates. It is likely that isotope ratios in the WS treatments were affected by near complete denitrification to N_2 . Well *et al.* (2012) observed highly variable isotopocule ratios in a strongly denitrifying aquifer and concluded that N_2O reduction was strongly progressed but variable. However, it should be noted that their system had abundant NO_3^- while ours did not. The inconsistent relationships between $\text{N}_2\text{O}_{\text{emitted}}$ and $\text{N}_2\text{O}_{\text{poreair}}$ for $\text{SP}/\delta^{15}\text{N}$ and $\text{SP}/\delta^{18}\text{O}$ in the WS treatments and the stronger enrichment observed in the DS-AWD $\text{N}_2\text{O}_{\text{emitted}}$ (Fig. 4) demonstrate a disconnection between subsurface $\text{N}_2\text{O}_{\text{emitted}}$ and $\text{N}_2\text{O}_{\text{poreair}}$ across treatments. Such results suggest that N_2O reduction may not have had as strong of an influence on the signature of $\text{N}_2\text{O}_{\text{emitted}}$ as it did on $\text{N}_2\text{O}_{\text{poreair}}$, particularly in the WS treatments. A de-coupling between subsurface N_2O concentrations and surface emissions, and their isotopocule ratios has been observed in other studies (Van Groenigen *et al.*, 2005; Goldberg *et al.*, 2010a). This phenomenon is most simply explained by emitted N_2O truly coming from a mix of sources and depths, while subsurface N_2O is representative of a much smaller spatial zone and more likely to be dominated by one process. While difficult to practically measure, processes at shallow depths above 5 cm, were also likely influential to surface emissions.

4.4 Complementary evidence from a two endmember mixing model approach

To quantitatively estimate the extent of N_2O reduction (gross $r\text{N}_2\text{O}$), N_2O production and reduction rates, and the contribution of denitrification to N_2O emissions, we used an open and closed system two endmember mixing model based on $\text{SP}-\text{N}_2\text{O}$ and $\delta^{18}\text{O}-\text{N}_2\text{O}$ relationships. As described in section 2.7, we tested our models under two scenarios; in scenario one (sc1) N_2O is produced and reduced by denitrifiers before mixing with N_2O derived from nitrification, in scenario two (sc2) N_2O is produced from both processes, mixed, and then reduced (Fig. 1). While we could estimate gross $r\text{N}_2\text{O}$ and the fraction of denitrification from both scenarios, sc2 yielded mostly implausible solutions for the contribution of denitrification to N_2O in open systems



(Fig. S3 and Table S2). We thus conclude that the assumptions underlying this scenario in open systems were not valid in our system. In a closed system N_2O is progressively consumed and not replenished, resulting in a stronger isotope effect and faster enrichment of the remaining N_2O ; thus a smaller degree of N_2O reduction is needed to achieve an equivalent enrichment as in open systems. Our results for open and closed systems align well with this theory on N_2O fractionation. Given the lower moisture and evidence of extensive nitrification occurring in the DS-AWD treatment, we expected a higher contribution of nitrification/fungal denitrification in this treatment, coming from an increase in nitrification. However, this was not the case and denitrification/nitrifier-denitrification contributions tended to be higher in the DS-AWD treatment relative to WS treatments (Fig. 5a, Fig. 6). Treatment differences were significant in the surface fluxes, however there was a significant interaction with sampling day; there was no treatment effect on denitrification contribution in the subsurface (Table 5). The equivalent or higher contributions of nitrification/fungal denitrification in the WS treatments (Fig. 6) are most easily explained by higher fungal denitrification; in their laboratory experiments, Lewicka-Szczebak *et al.* (2017) also observed relatively high fungal denitrification contributions under very wet conditions. Larger contributions from fungal denitrification would also help explain the less clear reduction trends as fungal denitrifiers are thought to largely produce N_2O as an end-product rather than N_2 . It should be noted that due to low surface fluxes or $\text{N}_2\text{O}_{\text{poreair}}$, we had fewer data points in the WS treatments. Previous studies have attributed significant amounts of N_2O emissions in paddy systems to nitrification in periods of low soil moisture (Lagomarsino *et al.*, 2016; Verhoeven *et al.*, 2018). Yet, such studies were not able to quantitatively source-partition emissions. Given our results here, it is possible that N_2O produced either via nitrifier-denitrification or coupled nitrification-denitrification has been previously underestimated.

The modeled gross $r\text{N}_2\text{O}$ fractions indicate high levels of N_2O reduction for all treatments and depths, ($r\text{N}_2\text{O}$: 0.06 to 0.19) even in the DS-AWD where soil moisture was frequently below 60% at 5 cm (Fig. 2). These results are at first surprising, but there is still much we do not know about subsurface N_2O production and consumption. Direct measurements of N_2O reduction at depth are few. Using membrane inlet mass spectrometry, Zhou *et al.* (2017) detected higher N_2O reduction to N_2 in paddy soil water at 20 cm versus 60 or 80 cm and could relate this to higher DOC concentrations at 20 cm. Other studies suggest high subsurface N_2O reduction based on the inference of declining N_2O concentration accompanied by isotope enrichment moving up a soil profile (Clough *et al.*, 1998; Van Groenigen *et al.*, 2005; Goldberg *et al.*, 2008). We are also methodologically limited by our inability to measure N_2O isotopocules at near, or complete N_2O reduction because there is too little remaining N_2O to measure. We assume this was more often the case in the WS treatments, therefore we postulate that the signature of N_2O reduction was stronger in the DS-AWD largely because there was more N_2O left to measure. In their experiments to validate the mixing model we used, Lewicka-Szczebak *et al.* (2017) found that the model routinely underestimated gross $r\text{N}_2\text{O}$ rates relative to measured rates in an oxic mineral soil, but performed better under anoxic conditions and in an organic soil. Therefore, an underestimation of $r\text{N}_2\text{O}$ rates, particularly in the DS-AWD treatments, remains possible. However, considering the strong indication of N_2O reduction from other isotopocule relationships (i.e. SP and $\delta^{15}\text{N}$ and $\delta^{15}\text{N}$ and $\delta^{18}\text{O}$) we believe that subsurface N_2O reduction rates were simply high in our system, regardless of water management.



In the subsurface, the contribution of denitrification/nitrifier-denitrification to N_2O concentrations was positively correlated to $\text{N}_2\text{O}_{\text{poreair}}$ concentrations and WFPS in all treatments, indicating an increasing contribution of denitrification/nitrifier-denitrification at times of higher N_2O production in conjunction with rising soil moisture (Table 6). In the two AWD treatments, the contribution of denitrification/nitrifier-denitrification negatively correlated to $\delta^{15}\text{N}$ signature of $\text{N}_2\text{O}_{\text{poreair}}$ and $\text{N}_2\text{O}_{\text{emitted}}$ (DS-AWD only). Many studies have demonstrated that high subsurface N_2O production is correlated to depleted $\delta^{15}\text{N}$ - N_2O (Van Groenigen *et al.*, 2005; Goldberg *et al.*, 2008; Goldberg *et al.*, 2010b). These results further support the conclusion that high $\text{N}_2\text{O}_{\text{poreair}}$ and $\text{N}_2\text{O}_{\text{emitted}}$ were produced from denitrification/nitrifier-denitrification associated with more depleted $\delta^{15}\text{N}$ - N_2O . Higher gross $r\text{N}_2\text{O}$ (less N_2O reduction) was associated with higher $\text{N}_2\text{O}_{\text{emitted}}$ in all treatments and higher $\text{N}_2\text{O}_{\text{poreair}}$ (WS-AWD only), demonstrating that higher N_2O resulted not only from increased denitrification/nitrifier-denitrification but also from a decrease in N_2O reduction. Interestingly, higher $r\text{N}_2\text{O}$ in $\text{N}_2\text{O}_{\text{emitted}}$ of the DS-AWD was also associated with higher WFPS. Such a result can only be explained by a dependency of reduction on N_2O production. Overall, there was a negative relationship between $r\text{N}_2\text{O}$ and $\delta^{15}\text{N}$ - N_2O , yet the relationship was not consistently strong or significant between treatments. A negative relationship supports an isotope enrichment effect with greater N_2O reduction. Considering the above, it appears that maximum N_2O production and emissions occurred during periods of increased contribution from denitrification/nitrifier-denitrification, which were accompanied by small declines in N_2O reduction. These relationships were most robust in the DS-AWD treatment. Correlations within the $\text{N}_2\text{O}_{\text{emitted}}$ dataset were undoubtedly affected by lower data availability, particularly in the WS treatments, and should be taken with caution. Despite the high estimates of N_2O reduction for all treatments, we still observed relevant contributions from nitrification/fungal denitrification on many dates (Fig. 6). Nevertheless, the highest fluxes in the DS-AWD aligned with higher contributions from denitrification/nitrifier-denitrification, while the highest fluxes in the WS treatment had nitrification/fungal denitrification contributions of ca. 50%. In the WS treatments we again postulate that fungal denitrification rates increased because conditions were not ideal for high nitrification. Studies have shown that fungal denitrification and co-denitrification can play a significant role in soil N_2 and N_2O emissions from soil (Laughlin and Stevens, 2002; Long *et al.*, 2013).

25

From our modeling results we could estimate N_2 production or emissions based on our calculated N_2O reduction rates (Fig.S13). Due to poor data availability and high variability we could neither confidently estimate N_2 production at 25 cm nor surface N_2 emissions on many dates of the WS treatments, but we have more confidence in the estimates obtained for the DS-AWD treatment. Mean daily N_2 emissions found in our study were 236 ± 53 (n=43), 194 ± 37 (n=41) and 197 ± 35 (n=31) g $\text{N ha}^{-1} \text{ d}^{-1}$ in the DS-AWD, WS-AWD and WS-FLD, respectively. To our knowledge only one other study by Yano *et al.* (2014) has conducted similar calculations to estimate N_2 emissions in rice systems from isotopocule signatures. The authors also found high rates of N_2O reduction, around 80 to 85%, corresponding to an $r\text{N}_2\text{O}$ of 0.15 to 0.20 and N_2 emissions between 0.1 to 422 $\mu\text{g N m}^2 \text{ hr}^{-1}$ (or 0.024 to 101.4 g $\text{ha}^{-1} \text{ d}^{-1}$). Therefore, the estimated extent of N_2O reduction was quite similar to our surface emitted reduction rates, with somewhat lower N_2 emissions corresponding to somewhat lower N_2O emissions.

30



Using labeled ^{15}N urea, Lindau *et al.* (1990) measured N_2 emissions of $254 \text{ g ha}^{-1} \text{ d}^{-1}$, while Dong *et al.* (2012) observed similar rates of $194 \text{ g N}_2\text{-N ha}^{-1} \text{ d}^{-1}$ for an AWD treatment. Considering that these results only account for N_2 derived from fertilizer, the modeled mean daily N_2 emissions found in our study are plausible. Differences between the treatment means were not significant for $\text{N}_2\text{O}_{\text{poreair}}$ or $\text{N}_2\text{O}_{\text{emitted}}$ ($p=0.431$ and $p=0.858$), thus do not indicate a higher potential for N_2 losses in the WS treatments. We must reject our hypothesis that higher NO_3^- in the WS-AWD relative to the WS-FLD would drive higher denitrification and N_2 losses because we observed no differences in final modeled N_2 production and NO_3^- concentrations were essentially null for both WS treatments. Our results show there is promise for estimating N_2 emissions from N_2O isotopocule signatures using simple models, but the precision of these estimates remains constrained by our ability to measure N_2O isotopocule signatures at low fluxes. Modeling efforts could also be refined through the implementation of a set of criteria (i.e. soil moisture status) to determine open versus closed system dynamics for a given sample.

5 Conclusions

The relatively dry conditions in the DS-AWD treatment and application of urea fertilizer led to extensive nitrification, subsequent denitrification and denitrification derived N_2O emissions. Even with evidence of nitrification and relatively aerobic conditions in the DS-AWD treatment, both graphical and two endmember mixing model results indicated significant N_2O reduction in all treatments and most convincingly in the DS-AWD treatment. Differences between depths were often more evident in $\text{N}_2\text{O}_{\text{poreair}}$, NO_3^- , NH_4^+ and DOC concentrations than in N_2O isotope signatures at the various depths, particularly for the WS treatments. In the DS-AWD treatment, isotope signatures of $\delta^{18}\text{O}\text{-N}_2\text{O}$ and SP values demonstrated notably lower values at 5 cm relative to other depths, mostly likely indicating higher N_2O production and less reduction in the upper layer. Overall, the highest N_2O production and emissions were associated with an increasing contribution from denitrification/nitrifier-denitrification accompanied by decreases in N_2O reduction in the AWD treatments. Our isotope data suggests that contributions from fungal denitrification to N_2O emissions may have increased in the WS-FLD treatment. The role of fungal denitrification in paddy rice systems should be further investigated with the use of fungal inhibitors. Surface emitted N_2O reduction rates were similar for all treatments, therefore our hypothesis of a greater potential for gaseous N_2 losses in the WS-AWD is refuted. Despite the difficulty in obtaining a full dataset for all treatments and the inherent spatiotemporal variability in the original measured fluxes, we came to good agreement with the magnitude of N_2 emissions reported from previous ^{15}N labeled fertilizer studies. Thus such methods do show promise for estimating N_2 emissions and closing N budgets, even without the $\delta^{15}\text{N}$ of N substrates. Model results would likely improve with controlled incubations to determine site-specific isotope effects. Particularly in saturated or partly saturated systems, future studies should probe the disconnection between subsurface and emitted N_2O isotopocules by employing methods that allow for larger subsurface spatial integration, such as the installation of long horizontal gas collection tubes. It appears that to effectively manage N losses in alternative water management paddy systems inhibition of nitrification is necessary, particularly very early in the growing season when N availability exceeds crop N demand.



Dataset availability

Verhoeven, Elizabeth. (2018). CastelloD'Agogna_waterMgmt2015,2016_dataset (Version 1.0) [Data set]. Zenodo.
<http://doi.org/10.5281/zenodo.1251895>

Acknowledgements

- 5 This work was financially supported by the Swiss National Science Foundation (40FA40_154246) through the Joint Programming Initiative on Agriculture, Food Security and Climate Change (FACCE-JPI). This work would not have been possible without the support and assistance of the staff at Ente Nazionale Risi in Castello D'Agogna, Italy, in particular Marco Romani, Elenora Miniotti and Daniele Tenni.

References

- 10 Agenzia Regionale per la Protezione dell'Ambiente-Lomardia: <http://www2.arpalombardia.it/siti/arpalombardia/meteo/richiesta-dati-misurati/Pagine/RichiestaDatiMisurati.aspx>
- Arth, I., and Frenzel, P.: Nitrification and denitrification in the rhizosphere of rice: the detection of processes by a new multi-channel electrode, *Biology and Fertility of Soils*, 31, 427-435, 10.1007/s003749900190, 2000.
- 15 Aulakh, M. S., Khera, T. S., Doran, J. W., and Bronson, K. F.: Denitrification, N₂O and CO₂ fluxes in rice-wheat cropping system as affected by crop residues, fertilizer N and legume green manure, *Biology and Fertility of Soils*, 34, 375-389, 10.1007/s003740100420, 2001.
- Baggs, E. M.: A review of stable isotope techniques for N₂O source partitioning in soils: recent progress, remaining challenges and future considerations, *Rapid Commun. Mass Spectrom.*, 22, 1664-1672, 10.1002/rcm.3456, 2008.
- Bremner, J., Blackmer, A., and Waring, S.: Formation of nitrous oxide and dinitrogen by chemical decomposition of hydroxylamine in soils, *Soil Biology and Biochemistry*, 12, 263-269, 1980.
- 20 Butterbach-Bahl, K., Baggs, E. M., Dannenmann, M., Kiese, R., and Zechmeister-Boltenstern, S.: Nitrous oxide emissions from soils: how well do we understand the processes and their controls?, *Philos. Trans. R. Soc. B-Biol. Sci.*, 368, 13, 10.1098/rstb.2013.0122, 2013.
- Cai, Z., Xing, G., Yan, X., Xu, H., Tsuruta, H., Yagi, K., and Minami, K.: Methane and nitrous oxide emissions from rice paddy fields as affected by nitrogen fertilisers and water management, *Plant and Soil*, 196, 7-14, 1997.
- 25 Casciotti, K. L., Sigman, D. M., Hastings, M. G., Bohlke, J. K., and Hilkert, A.: Measurement of the oxygen isotopic composition of nitrate in seawater and freshwater using the denitrifier method, *Analytical Chemistry*, 74, 4905-4912, 10.1021/ac020113w, 2002.
- Cassman, K. G., Peng, S., Olk, D. C., Ladha, J. K., Reichardt, W., Dobermann, A., and Singh, U.: Opportunities for increased nitrogen-use efficiency from improved resource management in irrigated rice systems, *Field Crop. Res.*, 56, 7-39, [http://dx.doi.org/10.1016/S0378-4290\(97\)00140-8](http://dx.doi.org/10.1016/S0378-4290(97)00140-8), 1998.
- Clough, T., Jarvis, S., Dixon, E., Stevens, R., Laughlin, R., and Hatch, D.: Carbon induced subsoil denitrification of 15 N-labelled nitrate in 1 m deep soil columns, *Soil Biology and Biochemistry*, 31, 31-41, 1998.
- 30 Decock, C., and Six, J.: How reliable is the intramolecular distribution of N-15 in N₂O to source partition N₂O emitted from soil?, *Soil Biology & Biochemistry*, 65, 114-127, 10.1016/j.soilbio.2013.05.012, 2013a.
- Decock, C., and Six, J.: On the potential of delta O-18 and delta N-15 to assess N₂O reduction to N-2 in soil, *European Journal of Soil Science*, 64, 610-620, 10.1111/ejss.12068, 2013b.



- Dedatta, S. K., Buresh, R. J., Samson, M. I., Obcemea, W. N., and Real, J. G.: DIRECT MEASUREMENT OF AMMONIA AND DENITRIFICATION FLUXES FROM UREA APPLIED TO RICE, *Soil Science Society of America Journal*, 55, 543-548, 1991.
- Denk, T. R., Mohn, J., Decock, C., Lewicka-Szczepak, D., Harris, E., Butterbach-Bahl, K., Kiese, R., and Wolf, B.: The nitrogen cycle: A review of isotope effects and isotope modeling approaches, *Soil Biology and Biochemistry*, 105, 121-137, 2017.
- 5 Devkota, K. P., Manschadi, A., Lamers, J. P. A., Devkota, M., and Vlek, P. L. G.: Mineral nitrogen dynamics in irrigated rice-wheat system under different irrigation and establishment methods and residue levels in arid drylands of Central Asia, *European Journal of Agronomy*, 47, 65-76, 10.1016/j.eja.2013.01.009, 2013.
- Doane, T. A., and Horwath, W. R.: Spectrophotometric determination of nitrate with a single reagent, *Analytical Letters*, 36, 2713-2722, 2003.
- 10 Dong, N. M., Brandt, K. K., Sørensen, J., Hung, N. N., Van Hach, C., Tan, P. S., and Dalsgaard, T.: Effects of alternating wetting and drying versus continuous flooding on fertilizer nitrogen fate in rice fields in the Mekong Delta, Vietnam, *Soil Biology and Biochemistry*, 47, 166-174, 2012.
- Firestone, M., Davidson, E., Andreae, M., and Schimel, D.: Microbiological basis of NO and N₂O production and consumption in soil, Exchange of trace gases between terrestrial ecosystems and the atmosphere., 7-21, 1989.
- Frame, C. H., and Casciotti, K.: Biogeochemical controls and isotopic signatures of nitrous oxide production by a marine ammonia-oxidizing bacterium, *Biogeosciences*, 7, 2695, 2010.
- 15 Fry, B.: *Stable isotope ecology*, Springer, 2007.
- Goldberg, S. D., Knorr, K.-H., and Gebauer, G.: N₂O concentration and isotope signature along profiles provide deeper insight into the fate of N₂O in soils†, *Isotopes in environmental and health studies*, 44, 377-391, 2008.
- Goldberg, S. D., Knorr, K.-H., Blodau, C., Lischeid, G., and Gebauer, G.: Impact of altering the water table height of an acidic fen on N₂O and NO fluxes and soil concentrations, *Global Change Biology*, 16, 220-233, 10.1111/j.1365-2486.2009.02015.x, 2010a.
- 20 Goldberg, S. D., KNORR, K. H., Blodau, C., Lischeid, G., and Gebauer, G.: Impact of altering the water table height of an acidic fen on N₂O and NO fluxes and soil concentrations, *Global change biology*, 16, 220-233, 2010b.
- Heil, J., Wolf, B., Brüggemann, N., Emmenegger, L., Tuzson, B., Vereecken, H., and Mohn, J.: Site-specific ¹⁵N isotopic signatures of abiotically produced N₂O, *Geochimica et Cosmochimica Acta*, 139, 72-82, 2014.
- 25 Heil, J., Liu, S., Vereecken, H., and Brüggemann, N.: Abiotic nitrous oxide production from hydroxylamine in soils and their dependence on soil properties, *Soil Biology and Biochemistry*, 84, 107-115, 2015.
- Hu, H.-W., Chen, D., and He, J.-Z.: Microbial regulation of terrestrial nitrous oxide formation: understanding the biological pathways for prediction of emission rates, *FEMS microbiology reviews*, 39, 729-749, 2015.
- Hutchinson, G., and Mosier, A.: Improved soil cover method for field measurement of nitrous oxide fluxes, *Soil Science Society of America Journal*, 45, 311-316, 1981.
- 30 IPCC: *IPCC Fourth Assessment Report: Climate Change 2007*. 2007.
- Jinuntuya-Nortman, M., Sutka, R. L., Ostrom, P. H., Gandhi, H., and Ostrom, N. E.: Isotopologue fractionation during microbial reduction of N₂O within soil mesocosms as a function of water-filled pore space, *Soil Biology and Biochemistry*, 40, 2273-2280, <https://doi.org/10.1016/j.soilbio.2008.05.016>, 2008.
- Kendall, C., and McDonnell, J. J.: *Isotope tracers in catchment hydrology*, Elsevier, 2012.
- 35 Koba, K., Osaka, K., Tobari, Y., Toyoda, S., Ohte, N., Katsuyama, M., Suzuki, N., Itoh, M., Yamagishi, H., and Kawasaki, M.: Biogeochemistry of nitrous oxide in groundwater in a forested ecosystem elucidated by nitrous oxide isotopomer measurements, *Geochimica et Cosmochimica Acta*, 73, 3115-3133, 2009.



- Koehler, B., Corre, M. D., Steger, K., Well, R., Zehe, E., Sueta, J. P., and Veldkamp, E.: An in-depth look into a tropical lowland forest soil: nitrogen-addition effects on the contents of N₂O, CO₂ and CH₄ and N₂O isotopic signatures down to 2-m depth, *Biogeochemistry*, 111, 695-713, 2012.
- Kool, D. M., Wrage, N., Oenema, O., Dolfing, J., and Van Groenigen, J. W.: Oxygen exchange between (de) nitrification intermediates and H₂O and its implications for source determination of NO₃⁻ and N₂O: a review, *Rapid Commun. Mass Spectrom.*, 21, 3569-3578, 10.1002/rcm.3249, 2007.
- 5 Kool, D. M., Wrage, N., Oenema, O., Harris, D., and Van Groenigen, J. W.: The O-18 signature of biogenic nitrous oxide is determined by O exchange with water, *Rapid Commun. Mass Spectrom.*, 23, 104-108, 10.1002/rcm.3859, 2009.
- Kool, D. M., Wrage, N., Zechmeister-Boltenstern, S., Pfeffer, M., Brus, D., Oenema, O., and Van Groenigen, J. W.: Nitrifier denitrification can be a source of N₂O from soil: a revised approach to the dual-isotope labelling method, *European Journal of Soil Science*, 61, 759-772, 10.1111/j.1365-2389.2010.01270.x, 2010.
- 10 Kool, D. M., Dolfing, J., Wrage, N., and Van Groenigen, J. W.: Nitrifier denitrification as a distinct and significant source of nitrous oxide from soil, *Soil Biology & Biochemistry*, 43, 174-178, 10.1016/j.soilbio.2010.09.030, 2011.
- Lachouani, P., Frank, A. H., and Wanek, W.: A suite of sensitive chemical methods to determine the $\delta^{15}\text{N}$ of ammonium, nitrate and total dissolved N in soil extracts, *Rapid Commun. Mass Spectrom.*, 24, 3615-3623, 2010.
- Lagomarsino, A., Agnelli, A. E., Linquist, B., Adviento-Borbe, M. A., Agnelli, A., Gavina, G., Ravaglia, S., and Ferrara, R. M.: Alternate wetting and drying of rice reduced CH₄ emissions but triggered N₂O peaks in a clayey soil of central Italy, *Pedosphere*, 26, 533-548, 2016.
- 15 Laughlin, R. J., and Stevens, R. J.: Evidence for fungal dominance of denitrification and codenitrification in a grassland soil, *Soil Science Society of America Journal*, 66, 1540-1548, 2002.
- Lewicka-Szczebak, D., Well, R., Koester, J. R., Fuss, R., Senbayram, M., Dittert, K., and Flessa, H.: Experimental determinations of isotopic fractionation factors associated with N₂O production and reduction during denitrification in soils, *Geochimica Et Cosmochimica Acta*, 134, 55-73, 10.1016/j.gca.2014.03.010, 2014.
- 20 Lewicka-Szczebak, D., Dyckmans, J., Kaiser, J., Marca, A., Augustin, J., and Well, R.: Oxygen isotope fractionation during N₂O production by soil denitrification, 2016.
- Lewicka-Szczebak, D., Augustin, J., Giesemann, A., and Well, R.: Quantifying N₂O reduction to N₂ based on N₂O isotopocules-validation with independent methods (helium incubation and ¹⁵N gas flux method), *Biogeosciences*, 14, 711, 2017.
- 25 Lide, D. R.: CRC handbook of chemistry and physics, CRC press, 2004.
- Lindau, C. W., Delaune, R. D., Patrick, W. H., and Bollich, P. K.: FERTILIZER EFFECTS ON DINITROGEN, NITROUS-OXIDE, AND METHANE EMISSIONS FROM LOWLAND RICE, *Soil Science Society of America Journal*, 54, 1789-1794, 1990.
- Long, A., Heitman, J., Tobias, C., Philips, R., and Song, B.: Co-occurring anammox, denitrification, and codenitrification in agricultural soils, *Applied and environmental microbiology*, 79, 168-176, 2013.
- 30 Maeda, K., Spor, A., Edel-Hermann, V., Heraud, C., Breuil, M.-C., Bizouard, F., Toyoda, S., Yoshida, N., Steinberg, C., and Philippot, L.: N₂O production, a widespread trait in fungi, *Scientific reports*, 5, 9697, 2015.
- Mariotti, A., Germon, J. C., Hubert, P., Kaiser, P., Letolle, R., Tardieux, A., and Tardieux, P.: Experimental determination of nitrogen kinetic isotope fractionation: Some principles; illustration for the denitrification and nitrification processes, *Plant and Soil*, 62, 413-430, 10.1007/bf02374138, 1981.
- McIlvin, M. R., and Casciotti, K. L.: Technical updates to the bacterial method for nitrate isotopic analyses, *Analytical chemistry*, 83, 1850-1856, 2011.
- 35 Miniotti, E. F., Romani, M., Said-Pullicino, D., Facchi, A., Bertora, C., Peyron, M., Sacco, D., Bischetti, G. B., Lerda, C., and Tenni, D.: Agro-environmental sustainability of different water management practices in temperate rice agro-ecosystems, *Agriculture, Ecosystems & Environment*, 222, 235-248, 2016.



- Mosier, A., Kroeze, C., Nevison, C., Oenema, O., Seitzinger, S., and van Cleemput, O.: Closing the global N₂O budget: nitrous oxide emissions through the agricultural nitrogen cycle, *Nutrient Cycling in Agroecosystems*, 52, 225-248, 1998.
- Ostrom, N. E., Pitt, A., Sutka, R., Ostrom, P. H., Grandy, A. S., Huizinga, K. M., and Robertson, G. P.: Isotopologue effects during N₂O reduction in soils and in pure cultures of denitrifiers, *Journal of Geophysical Research: Biogeosciences*, 112, 2007.
- 5 Ostrom, N. E., and Ostrom, P. H.: The Isotopomers of Nitrous Oxide: Analytical Considerations and Application to Resolution of Microbial Production Pathways, *Handbook of Environmental Isotope Geochemistry*, Vols 1 and 2, edited by: Baskaran, M., 453-476 pp., 2011.
- Peyron, M., Bertora, C., Pelissetti, S., Said-Pullicino, D., Celi, L., Miniotti, E., Romani, M., and Sacco, D.: Greenhouse gas emissions as affected by different water management practices in temperate rice paddies, *Agriculture, Ecosystems & Environment*, 232, 17-28, 2016.
- 10 Rapti-Caputo, D., and Martinelli, G.: The geochemical and isotopic composition of aquifer systems in the deltaic region of the Po River plain (northern Italy), *Hydrogeology journal*, 17, 467-480, 2009.
- Ratering, S., and Schnell, S.: Localization of iron-reducing activity in paddy soil by profile studies, *Biogeochemistry*, 48, 341-365, 2000.
- Ravishankara, A. R., Daniel, J. S., and Portmann, R. W.: Nitrous Oxide (N₂O): The Dominant Ozone-Depleting Substance Emitted in the 21st Century, *Science*, 326, 123-125, [10.1126/science.1176985](https://doi.org/10.1126/science.1176985), 2009.
- 15 Röckmann, T., Kaiser, J., Brenninkmeijer, C. A., and Brand, W. A.: Gas chromatography/isotope-ratio mass spectrometry method for high-precision position-dependent ¹⁵N and ¹⁸O measurements of atmospheric nitrous oxide, *Rapid Commun. Mass Spectrom.*, 17, 1897-1908, 2003.
- Rohe, L., Anderson, T. H., Braker, G., Flessa, H., Giesemann, A., Lewicka-Szczepak, D., Wrage-Mönnig, N., and Well, R.: Dual isotope and isotopomer signatures of nitrous oxide from fungal denitrification—a pure culture study, *Rapid Commun. Mass Spectrom.*, 28, 1893-1903, 2014.
- Said-Pullicino, D., Miniotti, E. F., Sodano, M., Bertora, C., Lerda, C., Chiaradia, E. A., Romani, M., Cesari de Maria, S., Sacco, D., and Celi, L.: Linking dissolved organic carbon cycling to organic carbon fluxes in rice paddies under different water management practices, *Plant and Soil*, 401, 273-290, [10.1007/s11104-015-2751-7](https://doi.org/10.1007/s11104-015-2751-7), 2016.
- 20 Schreiber, F., Wunderlin, P., Udert, K. M., and Wells, G. F.: Nitric oxide and nitrous oxide turnover in natural and engineered microbial communities: biological pathways, chemical reactions, and novel technologies, *Frontiers in microbiology*, 3, 2012.
- Seo, D. C., and DeLaune, R.: Fungal and bacterial mediated denitrification in wetlands: influence of sediment redox condition, *Water research*, 44, 2441-2450, 2010.
- 25 Sigman, D. M., Casciotti, K. L., Andreani, M., Barford, C., Galanter, M., and Bohlke, J. K.: A bacterial method for the nitrogen isotopic analysis of nitrate in seawater and freshwater, *Analytical Chemistry*, 73, 4145-4153, [10.1021/ac010088e](https://doi.org/10.1021/ac010088e), 2001.
- Smith, P., Martino, D., Cai, Z., Gwary, D., Janzen, H., Kumar, P., McCarl, B., Ogle, S., O'Mara, F., Rice, C., Scholes, B., Sirotenko, O., Howden, M., McAllister, T., Pan, G., Romanenkov, V., Schneider, U., Towprayoon, S., Wattenbach, M., and Smith, J.: Greenhouse gas mitigation in agriculture, *Philos. Trans. R. Soc. B-Biol. Sci.*, 363, 789-813, [10.1098/rstb.2007.2184](https://doi.org/10.1098/rstb.2007.2184), 2008.
- 30 Snider, D. M., Schiff, S. L., and Spoelstra, J.: ¹⁵N/ ¹⁴N and ¹⁸O/ ¹⁶O stable isotope ratios of nitrous oxide produced during denitrification in temperate forest soils, *Geochimica et Cosmochimica Acta*, 73, 877-888, [10.1016/j.gca.2008.11.004](https://doi.org/10.1016/j.gca.2008.11.004), 2009.
- Snider, D. M., Venkiteswaran, J. J., Schiff, S. L., and Spoelstra, J.: Deciphering the oxygen isotope composition of nitrous oxide produced by nitrification, *Global Change Biology*, 18, 356-370, 2012.
- 35 Snider, D. M., Venkiteswaran, J. J., Schiff, S. L., and Spoelstra, J.: A new mechanistic model of δ ¹⁸O N₂O formation by denitrification, *Geochimica et Cosmochimica Acta*, 112, 102-115, 2013.
- Stephan, K., and Kavanagh, K.: Suitability of the Diffusion Method for Natural Abundance Nitrogen-15 Analysis, *Soil Science Society of America Journal*, 73, 293, 2009.



- Sutka, R. L., Ostrom, N., Ostrom, P., Breznak, J., Gandhi, H., Pitt, A., and Li, F.: Distinguishing nitrous oxide production from nitrification and denitrification on the basis of isotopomer abundances, *Applied and environmental microbiology*, 72, 638-644, 2006.
- Sutka, R. L., Adams, G. C., Ostrom, N. E., and Ostrom, P. H.: Isotopologue fractionation during N₂O production by fungal denitrification, *Rapid Commun. Mass Spectrom.*, 22, 3989-3996, 2008.
- 5 Toyoda, S., Yano, M., Nishimura, S. i., Akiyama, H., Hayakawa, A., Koba, K., Sudo, S., Yagi, K., Makabe, A., and Tobari, Y.: Characterization and production and consumption processes of N₂O emitted from temperate agricultural soils determined via isotopomer ratio analysis, *Global Biogeochemical Cycles*, 25, 2011.
- USDA-NRCS: Keys to Soil Taxonomy, 11th ed. , USDA-Natural Resources Conservation Service, Washington, DC., 2010.
- 10 Van Groenigen, J. W., Zwart, K. B., Harris, D., and van Kessel, C.: Vertical gradients of delta N-15 and delta(18O) in soil atmospheric N₂O-temporal dynamics in a sandy soil, *Rapid Commun. Mass Spectrom.*, 19, 1289-1295, 10.1002/rcm.1929, 2005.
- Venterea, R. T., Halvorson, A. D., Kitchen, N., Liebig, M. A., Cavigelli, M. A., Grosso, S. J. D., Motavalli, P. P., Nelson, K. A., Spokas, K. A., and Singh, B. P.: Challenges and opportunities for mitigating nitrous oxide emissions from fertilized cropping systems, *Frontiers in Ecology and the Environment*, 10, 562-570, 2012.
- 15 Verhoeven, E., Pereira, E., Decock, C., Garland, G., Kennedy, T., Suddick, E., Horwath, W. R., and Six, J.: N₂O emissions from California farmlands: A review, *California Agriculture*, 71, 148-159, 10.3733/ca.2017a0026, 2017.
- Verhoeven, E., Decock, C., Barthel, M., Bertora, C., Sacco, D., Romani, M., Sleutel, S., and Six, J.: Nitrification and coupled nitrification-denitrification at shallow depths are responsible for early season N₂O emissions under alternate wetting and drying management in an Italian rice paddy system, *Soil Biology and Biochemistry*, 120, 58-69, <https://doi.org/10.1016/j.soilbio.2018.01.032>, 2018.
- Weiss, R., and Price, B.: Nitrous oxide solubility in water and seawater, *Marine Chemistry*, 8, 347-359, 1980.
- 20 Well, R., and Flessa, H.: Isotopologue enrichment factors of N₂O reduction in soils, *Rapid Commun. Mass Spectrom.*, 23, 2996-3002, 2009.
- Well, R., Eschenbach, W., Flessa, H., von der Heide, C., and Weymann, D.: Are dual isotope and isotopomer ratios of N₂O useful indicators for N₂O turnover during denitrification in nitrate-contaminated aquifers?, *Geochimica et cosmochimica acta*, 90, 265-282, 2012.
- Wilhelm, E., Battino, R., and Wilcock, R. J.: Low-pressure solubility of gases in liquid water, *Chemical reviews*, 77, 219-262, 1977.
- 25 Wolf, B., Merbold, L., Decock, C., Tuzson, B., Harris, E., Six, J., Emmenegger, L., and Mohn, J.: First on-line isotopic characterization of N₂O above intensively managed grassland, *Biogeosciences*, 12, 2517-2531, 2015.
- Wrage, N., Velthof, G., Van Beusichem, M., and Oenema, O.: Role of nitrifier denitrification in the production of nitrous oxide, *Soil biology and Biochemistry*, 33, 1723-1732, 2001.
- Wu, D., Köster, J. R., Cárdenas, L. M., Brüggemann, N., Lewicka-Szczebak, D., and Bol, R.: N₂O source partitioning in soils using ¹⁵N site preference values corrected for the N₂O reduction effect, *Rapid Commun. Mass Spectrom.*, 30, 620-626, 2016.
- 30 Xu, Y., Ge, J., Tian, S., Li, S., Nguy-Robertson, A. L., Zhan, M., and Cao, C.: Effects of water-saving irrigation practices and drought resistant rice variety on greenhouse gas emissions from a no-till paddy in the central lowlands of China, *Science of The Total Environment*, 505, 1043-1052, 2015.
- Yano, M., Toyoda, S., Tokida, T., Hayashi, K., Hasegawa, T., Makabe, A., Koba, K., and Yoshida, N.: Isotopomer analysis of production, consumption and soil-to-atmosphere emission processes of N₂O at the beginning of paddy field irrigation, *Soil Biology & Biochemistry*, 70, 66-78, 10.1016/j.soilbio.2013.11.026, 2014.
- 35 Yao, S.-H., Zhang, B., and Hu, F.: Soil biophysical controls over rice straw decomposition and sequestration in soil: the effects of drying intensity and frequency of drying and wetting cycles, *Soil Biology and Biochemistry*, 43, 590-599, 2011.
- Zhou, W., Xia, L., and Yan, X.: Vertical distribution of denitrification end-products in paddy soils, *Science of The Total Environment*, 576, 462-471, 2017.



Zhou, Z., Takaya, N., Sakairi, M. A. C., and Shoun, H.: Oxygen requirement for denitrification by the fungus *Fusarium oxysporum*, *Archives of Microbiology*, 175, 19-25, 2001.

Zhu-Barker, X., Cavazos, A. R., Ostrom, N. E., Horwath, W. R., and Glass, J. B.: The importance of abiotic reactions for nitrous oxide production, *Biogeochemistry*, 126, 251-267, 2015.

- 5 Zou, Y., Hirono, Y., Yanai, Y., Hattori, S., Toyoda, S., and Yoshida, N.: Isotopomer analysis of nitrous oxide accumulated in soil cultivated with tea (*Camellia sinensis*) in Shizuoka, central Japan, *Soil Biology and Biochemistry*, 77, 276-291, 2014.

Figure and table captions

Figure 1. Mapping approach scheme used in the closed system modeling. Adapted from (Lewicka-Szczebak et al., 2017).

- Figure 2.** N_2O surface emissions, \log_{10} of dissolved and pore air N_2O concentrations and major N_2O driving variables (NH_4^+ , NO_3^- , DOC, Eh, WFPS) throughout the field measurement period in the three water management treatments (WS-FLD = water-seeding + conventional flooding; WS-AWD = water-seeding + alternate wetting and drying; DS-AWD = direct dry seeding + alternate wetting and drying). The dashed vertical line indicates the date of fertilization (60 kg urea-N ha^{-1}). Blue shaded areas represent periods of flooding, shaded areas that last only one day indicate a ‘flush irrigation’ = flooding for < 6 hrs. The error bars represent the standard error of the mean.

- 15 **Figure 3.** Time course of $\delta^{15}\text{N}-\text{N}_2\text{O}$, $\delta^{18}\text{O}-\text{N}_2\text{O}$ and SP- N_2O in $\text{N}_2\text{O}_{\text{emitted}}$ and $\text{N}_2\text{O}_{\text{poreair}}$ across the three depths and water management treatments (WS-FLD = water-seeding + conventional flooding; WS-AWD = water-seeding + alternate wetting and drying; DS-AWD = direct dry seeding + alternate wetting and drying). The errors bars represent the standard error of the mean.

- Figure 4.** Graphical two-end member mixing plot after Lewicka-Szczebak *et al.* (2017) where sample values are plotted in SP x $\delta^{18}\text{O}-\text{N}_2\text{O}$ space (A) and two-end mixing plot after Toyoda *et al.* (2011) where sample values are plotted in SP x $\delta^{15}\text{N}-\text{N}_2\text{O}$ space (B). In panel (a) the black dots indicate the mean literature end-member values used in our modeling scenarios and the boxes represent a range of values derived from the literature attributed to each process, see section 2.7 and Table 2. To calculate the range of N_2O potentially produced by nitrification or denitrification in (B) we used the mean isotope effects, $\epsilon^{15}\text{N}_{\text{N}_2\text{O}/\text{NO}_3}$ and $\epsilon^{15}\text{N}_{\text{N}_2\text{O}/\text{NH}_4}$, reported in Denk *et al.* (2017) to represent denitrification and nitrification derived N_2O , respectively, and then added the minimum and maximum $\delta^{15}\text{N}-\text{NO}_3^-$ and $\delta^{15}\text{N}-\text{NH}_4^+$ values observed in each treatment (Supplementary Table 1.4). The linear relationship between each isotopocule pair is indicated in italics for all points together and for $\text{N}_2\text{O}_{\text{poreair}}$ only. The three water management treatments were: WS-FLD = water-seeding + conventional flooding; WS-AWD = water-seeding + alternate wetting and drying; DS-AWD = direct dry seeding + alternate wetting and drying.

- Figure 5.** Modeled denitrification/nitrifier-denitrification contribution and gross $r\text{N}_2\text{O}$ of open (grey bars), closed (blue bars) and mean (purple points and line) systems predicted by a two-endmember mixing model using $\delta^{18}\text{O}-\text{N}_2\text{O}$ and SP values. For open and closed system dynamics, the shaded bars represent the standard deviation range for each treatment x depth combination. The purple error bars represent the standard deviation around the mean.



Figure 6. Estimated contribution of denitrification/nitrifier-denitrification and nitrification/fungal denitrification to N_2O surface emissions in the three water management treatments (WS-FLD = water-seeding + conventional flooding; WS-AWD = water-seeding + alternate wetting and drying; DS-AWD = direct dry seeding + alternate wetting and drying). Estimates were derived from the mean of open and closed dynamics in a two endmember mixing model using $\delta^{18}\text{O}-\text{N}_2\text{O}$ and SP values.

Figure 7. Relationship of $\delta^{18}\text{O}-\text{NO}_3^-$ to $\delta^{15}\text{N}-\text{NO}_3^-$ in pore water samples of the three water management treatments (WS-FLD = water-seeding + conventional flooding; WS-AWD = water-seeding + alternate wetting and drying; DS-AWD = direct dry seeding + alternate wetting and drying). After Kendall and McDonnell (2012). The black arrow represents the trajectory of NO_3^- reduction effects. The black asterisk signifies the $\delta^{18}\text{O}$ value atmospheric O_2 (25.3 ‰) while the dashed black line indicates the range of $\delta^{18}\text{O}$ in soil water. $\delta^{18}\text{O}-\text{H}_2\text{O}$ was not directly measured in our study. We assumed a value of -8.3‰ taken from an uncontained aquifer in the region by Rapti-Caputo and Martinelli (2009). The symbol colors indicate the concentration of NO_3^- in each sample (mg L^{-1}).

Table 1. Dates of management activities during the experimental period in the three water management treatments (WS-FLD = water-seeding + conventional flooding; WS-AWD = water-seeding + alternate wetting and drying; DS-AWD = direct dry seeding + alternate wetting and drying).

Table 2. Endmember values used for modeling of the fraction of residual N_2O not reduced (gross $r\text{N}_2\text{O}$) and the fraction of $\text{N}_2\text{O} + \text{N}_2$ attributed to denitrification (gross frac_{DEN}) for both open and closed N_2O reduction fractionation dynamics.

Table 3. Spearman correlations of $\text{N}_2\text{O}_{\text{emitted}}$ with $\text{N}_2\text{O}_{\text{emitted}}$ isotopocule values, N_2O driving variables and $\text{N}_2\text{O}_{\text{poreair}}$ isotopocule values measured at 5 cm in the three water management treatments (WS-FLD = water-seeding + conventional flooding; WS-AWD = water-seeding + alternate wetting and drying; DS-AWD = direct dry seeding + alternate wetting and drying).

Significance indicated by: **** < 0.0001 , *** < 0.001 , ** < 0.01 , * < 0.05

Table 4. Spearman correlations between $\delta^{15}\text{N}-\text{NO}_3^-$ and $\delta^{15}\text{N}-\text{NH}_4^+$ with $\text{N}_2\text{O}_{\text{poreair}}$ concentration, $\delta^{15}\text{N}-\text{N}_2\text{O}_{\text{poreair}}$, NO_3^- and NH_4^+ concentrations in the three water management treatments (WS-FLD = water-seeding + conventional flooding; WS-AWD = water-seeding + alternate wetting and drying; DS-AWD = direct dry seeding + alternate wetting and drying).

Table 5. ANCOVA results of modeled residual N_2O not reduced (gross $r\text{N}_2\text{O}$), fraction of total $\text{N}_2 + \text{N}_2\text{O}$ production coming from denitrification (gross frac_{DEN}) and the fraction of N_2O attributed to denitrification (DenContribution) derived from $\text{N}_2\text{O}_{\text{emitted}}$ and $\text{N}_2\text{O}_{\text{poreair}}$. The Y position was used a co-variate and represents the longitudinal position of each replicate within field.

Table 6. Spearman correlations between modeled $r\text{N}_2\text{O}$ -gross, frac_{DEN} -gross and DenContribution with soil environmental variables and inorganic N substrates and $\delta^{15}\text{N}-\text{N}_2\text{O}$. Results are for the mean of open and closed system dynamics. Subsurface correlations were performed on data aggregated across 5 and 12.5 cm depths. Significance indicated by: **** < 0.0001 , *** < 0.001 , ** < 0.01 , * < 0.05

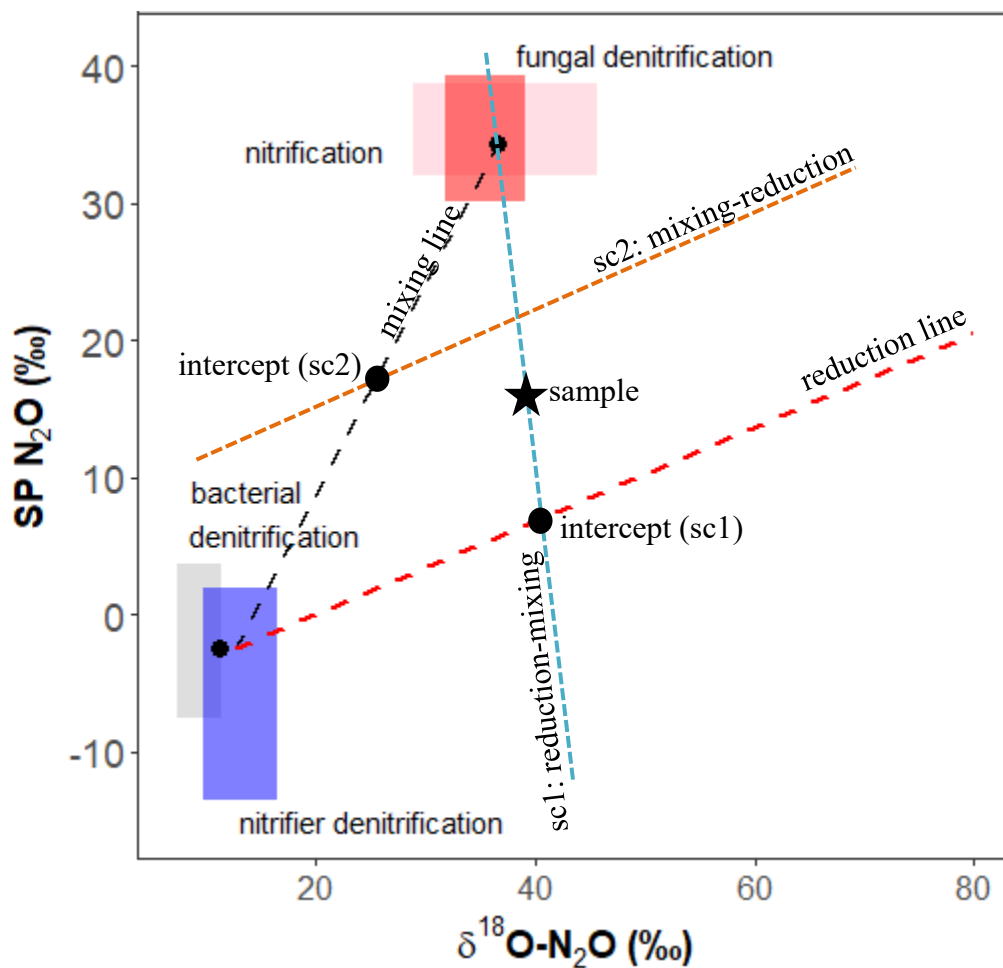


Figure 1.

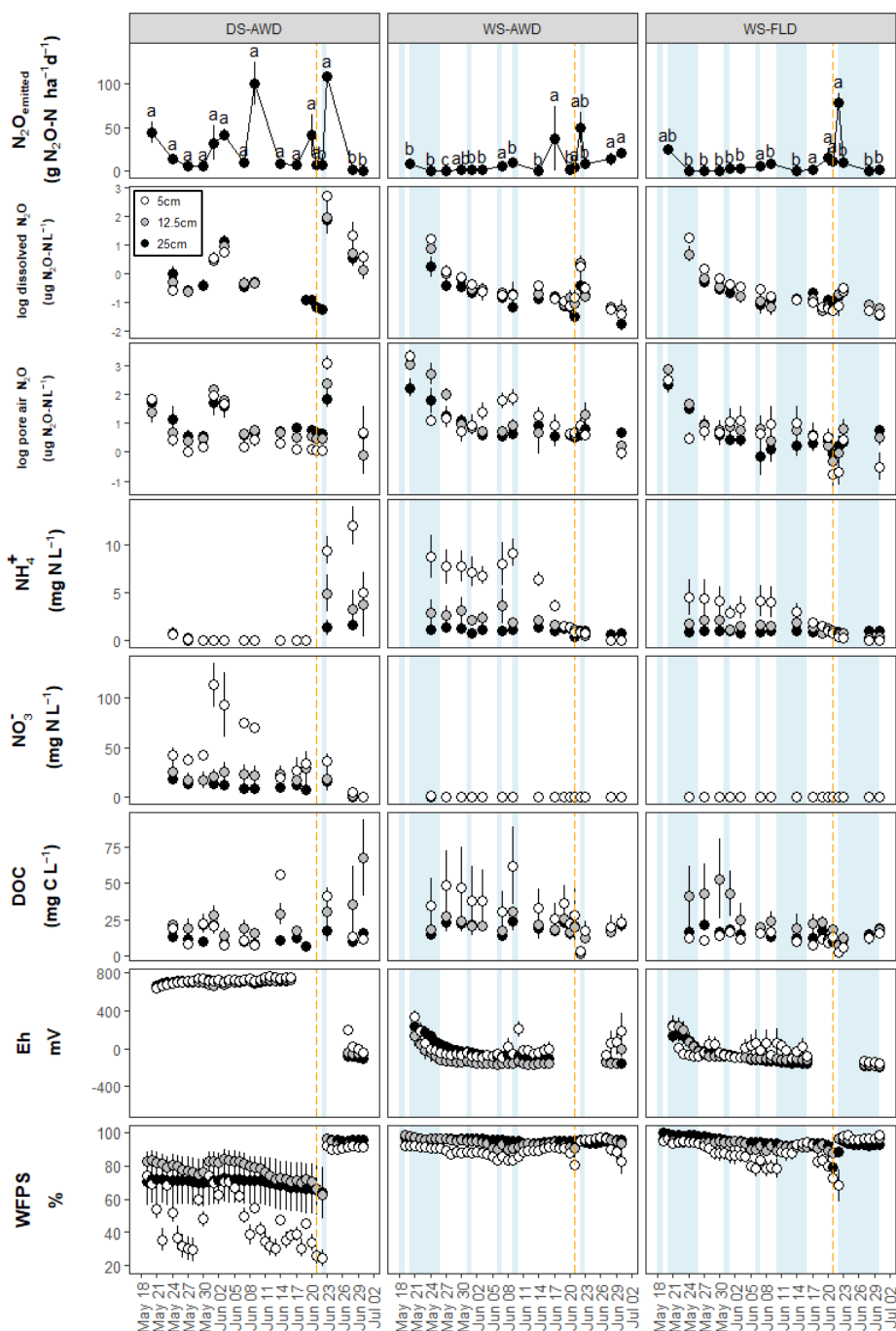


Figure 2.

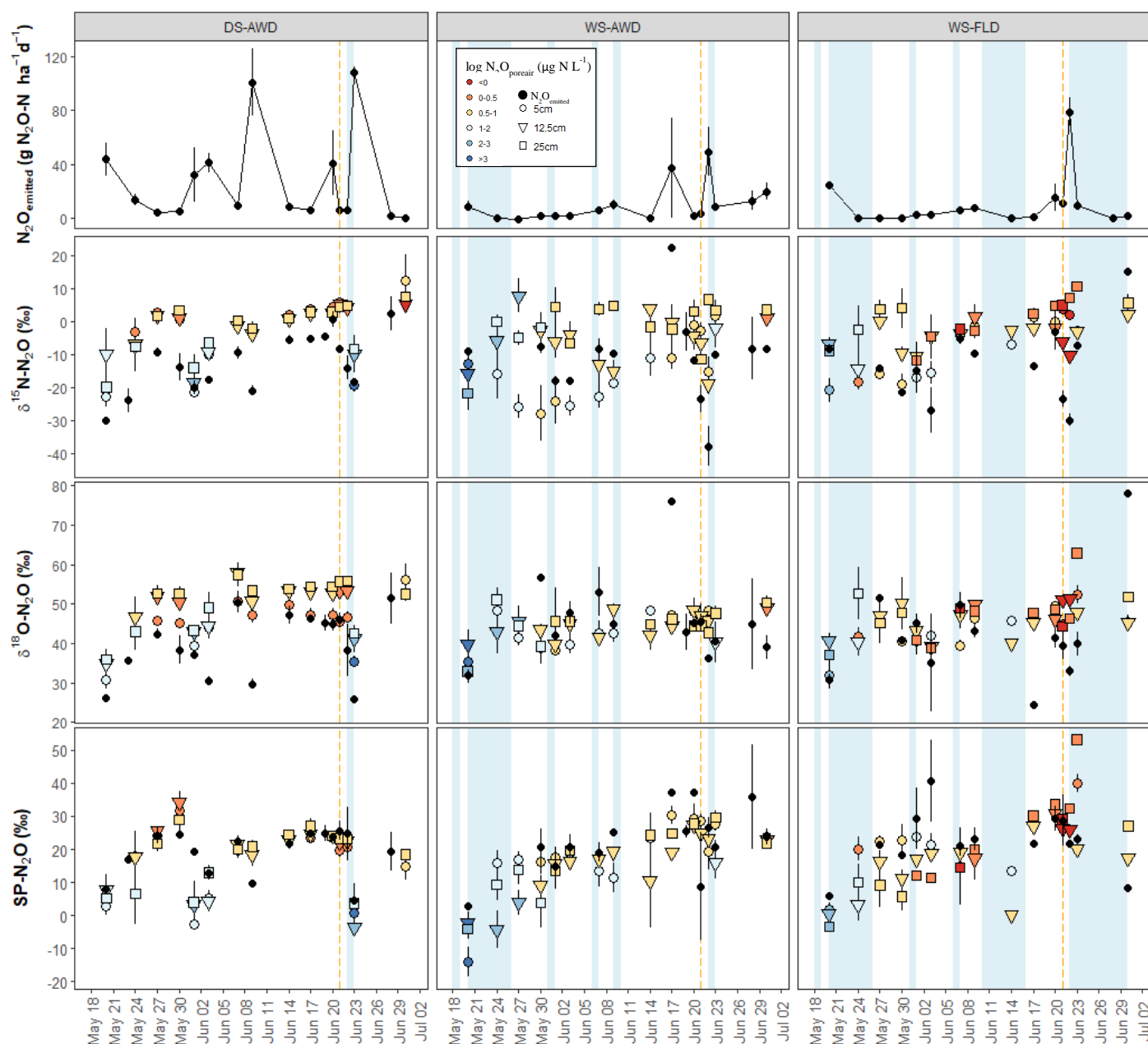


Figure 3.

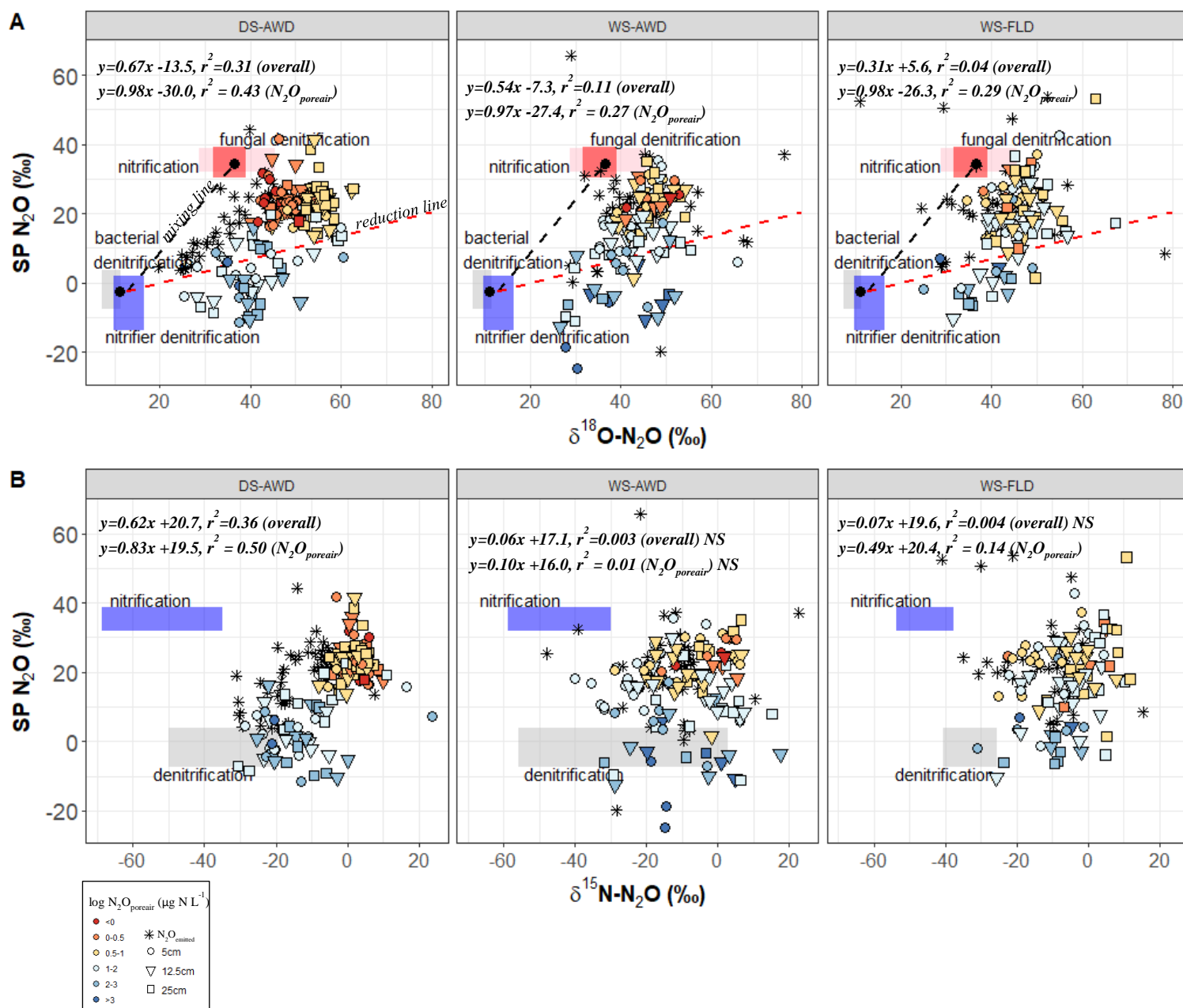
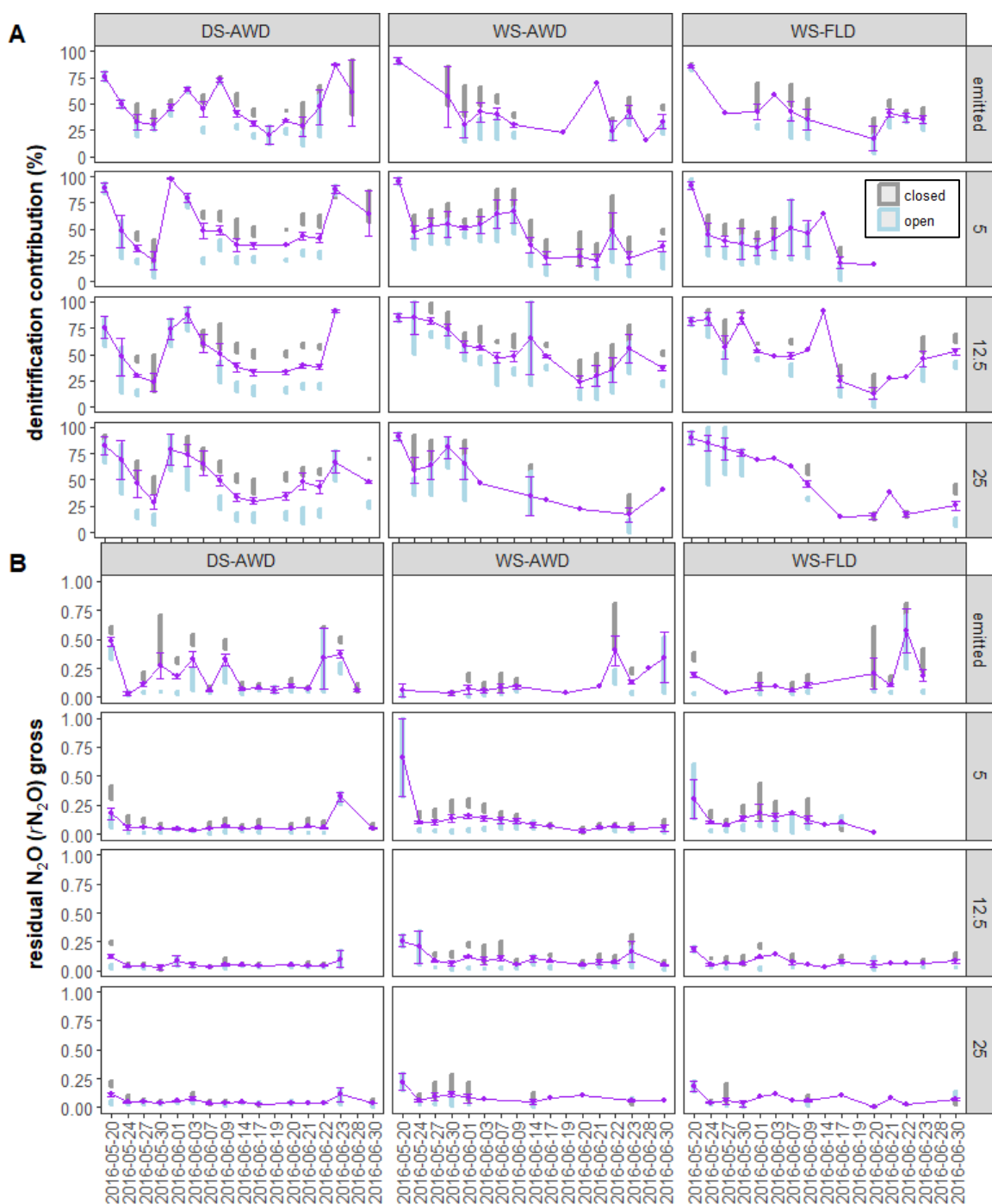


Figure 4.



5 Figure 5.

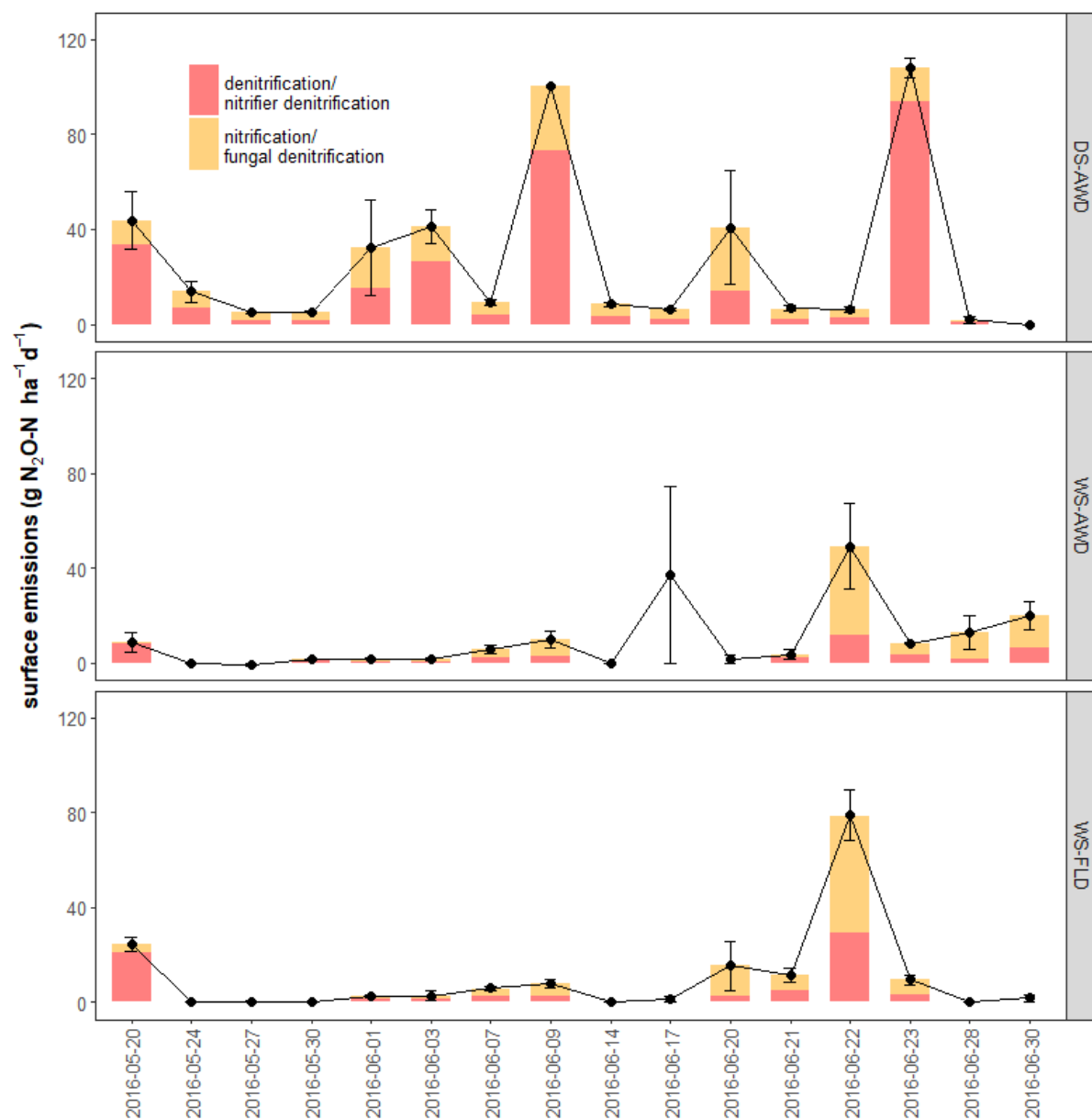


Figure 6.

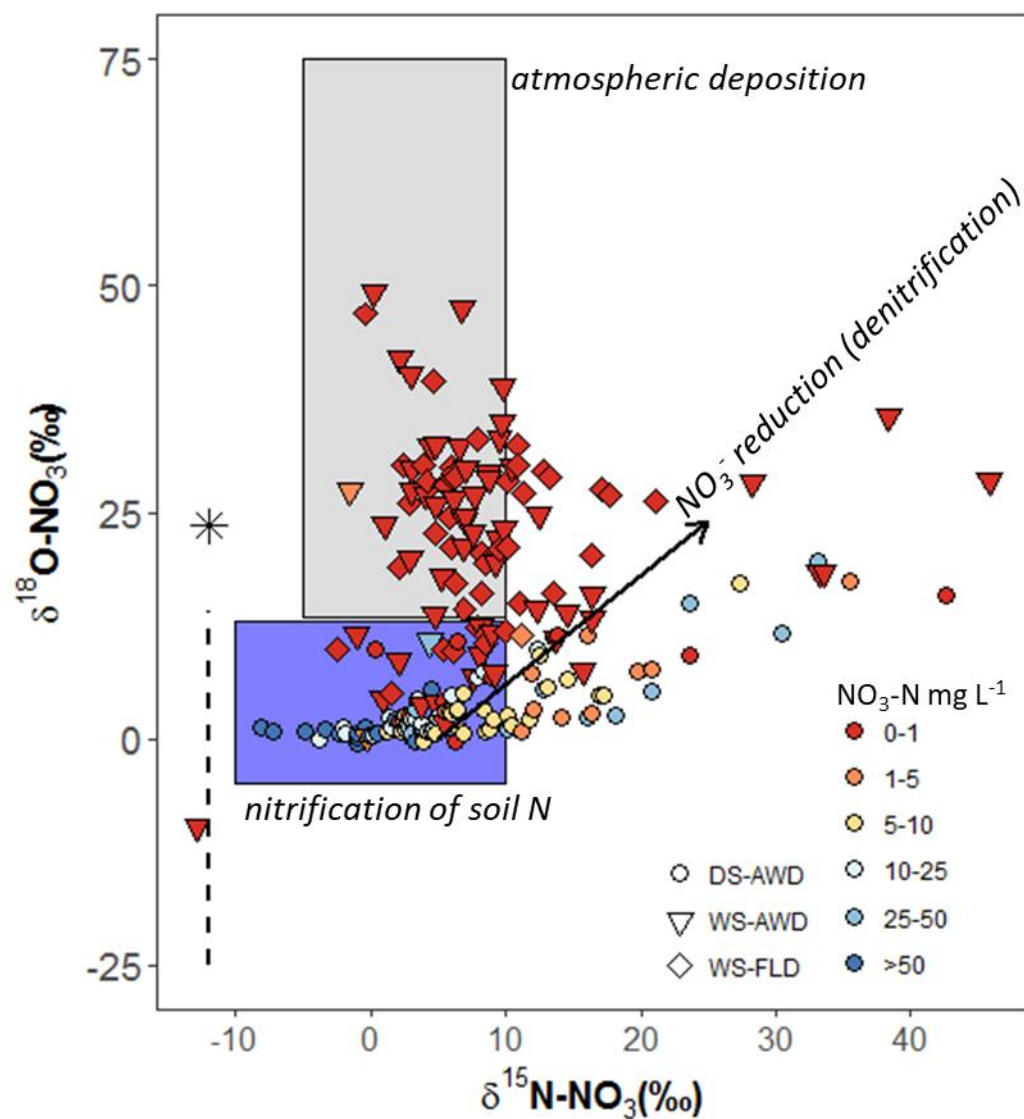


Figure 7.



Table 1. Dates of management activities during the experimental period in the three water management treatments (WS-FLD = water-seeding + conventional flooding; WS-AWD = water-seeding + alternate wetting and drying; DS-AWD = direct dry seeding + alternate wetting and drying).

Management	WS-FLD	WS-AWD	DS-AWD
ploughing; leveling	4-Apr; 12-Apr	4-Apr; 12-Apr	4-Apr; 12-Apr
Fertilization P-K	13-May (14-28 kg ha ⁻¹)	13-May (14-28 kg ha ⁻¹)	13-May (14-28 kg ha ⁻¹)
Fertilization N	16-May (60 kg ha ⁻¹)	16-May (60 kg ha ⁻¹)	16-May (40 kg ha ⁻¹)
Flooding	19-May	19-May	
Seeding	20-May	20-May	17-May
Drainage	26-May	26-May	
Flush irrigation	31-May;6-Jun	31-May;6-Jun;10-Jun	
Flooding	10-Jun		
Drainage	16-Jun		
Fertilization N	21-Jun (60 kg ha ⁻¹)	21-Jun (60 kg ha ⁻¹)	21-Jun (70 kg ha ⁻¹)
Flooding	22-Jun		
Flush irrigation		22-Jun	22-Jun
...			
Harvest	15-Sep	15-Sep	15-Sep



Table 2. Endmember values used for modeling of the fraction of residual N_2O not reduced (gross rN_2O) and the fraction of $N_2O + N_2$ attributed to denitrification (gross $frac_{DEN}$) for both open and closed N_2O reduction fractionation dynamics.

Process(s)	$\delta^{18}O-N_2O_{(x)}$	$SP_{(x)}$	references
denitrification, nitrifier-denitrification	12.7	-3.9	$\delta^{18}O$ and SP : Lewicka-Szczebak <i>et al.</i> (2017) * $\delta^{18}O$ uncorrected for $\delta^{18}O-H_2O$
nitrification, fungal denitrification	36.5	34.8	SP : Lewicka-Szczebak <i>et al.</i> (2017); $\delta^{18}O$: Sutka <i>et al.</i> (2006); Sutka <i>et al.</i> (2008); Frame and Casciotti (2010); Heil <i>et al.</i> (2014); Rohe <i>et al.</i> (2014); Maeda <i>et al.</i> (2015)
	$\epsilon^{18}O_{red}$	ϵSP_{red}	
N_2O reduction	-15	-5	Lewicka-Szczebak <i>et al.</i> (2017)

*Lewicka-Szczebak *et al.* (2017) originally report $\delta_0^{18}O-N_2O(N_2O/H_2O)$. Thus, to calculate a pure $\delta_0^{18}O-N_2O$, we added the $\delta^{18}O-H_2O$ value used in our study, -8.3‰.

Table 3. Spearman correlations of $N_2O_{emitted}$ with $N_2O_{emitted}$ isotopocule values, N_2O driving variables and $N_2O_{poreair}$ isotopocule values measured at 5 cm in the three water management treatments (WS-FLD = water-seeding + conventional flooding; WS-AWD = water-seeding + alternate wetting and drying; DS-AWD = direct dry seeding + alternate wetting and drying). Significance indicated by: **** <0.0001 , *** <0.001 , ** <0.01 , * <0.05

	$N_2O_{emitted}$			$\delta^{15}N-N_2O_{emitted}$			$\delta^{18}O-N_2O_{emitted}$			$\delta SP-N_2O_{emitted}$		
	WS-FLD	WS-AWD	DS-AWD	WS-FLD	WS-AWD	DS-AWD	WS-FLD	WS-AWD	DS-AWD	WS-FLD	WS-AWD	DS-AWD
$N_2O_{emitted}$				-0.16	0.03	-0.51***	-0.46**	-0.45**	-0.58****	-0.42*	0.36*	-0.68****
$N_2O_{dissolved, 5cm}$	-0.25	0.01	0.36	0.07	-0.39*	-0.3	0.14	-0.15	-0.56*	-0.07	0.21	-0.58*
$N_2O_{poreair, 5cm}$	0.00	-0.05	0.48***	0.11	0.15	-0.60****	-0.29	-0.11	-0.64****	-0.3	-0.32	-0.64****
WFPS _{5cm}	-0.23	-0.02	0.31*	0.25	-0.02	-0.49***	-0.09	-0.29	-0.50****	-0.22	-0.3	-0.64****
Eh _{5cm}	-0.03	0.15	0.25	0.05	-0.09	0.15	-0.03	-0.29	0.26	-0.02	0.44*	0.22
DOC _{5cm}	-0.08	-0.43**	-0.05	0.2	0.43**	0.13	0.40*	0.28	-0.03	-0.33	0.06	-0.03
$NO_3-N_{porewater, 5cm}$	-0.21	0.1	0.52***	-0.25	-0.29	-0.64****	-0.23	-0.15	-0.27	-0.13	-0.11	-0.21
$NH_4-N_{porewater, 5cm}$	-0.29*	-0.32*	-0.31	0.05	-0.02	0.23	0.29	0.43**	0.01	0.07	-0.16	-0.03
$\delta^{15}N-N_2O_{poreair, 5cm}$	0.24	0.09	-0.51****	-0.02	0.07	0.71****	0.1	-0.24	0.64****	0.1	0.1	0.65****
$\delta^{18}O-N_2O_{poreair, 5cm}$	-0.07	0.07	-0.39**	-0.13	-0.1	0.46***	0.02	-0.03	0.48***	0.33	0.47**	0.41**
$\delta SP-N_2O_{poreair, 5cm}$	-0.27	-0.1	-0.55****	0.18	-0.22	0.62****	0.14	0.21	0.49***	0.47*	0.55**	0.67****



Table 4. Spearman correlations between $\delta^{15}\text{N-NO}_3^-$ and $\delta^{15}\text{N-NH}_4^+$ with $\text{N}_2\text{O}_{\text{poreair}}$ concentration, $\delta^{15}\text{N-N}_2\text{O}_{\text{poreair}}$, NO_3^- and NH_4^+ concentrations in the three water management treatments (WS-FLD = water-seeding + conventional flooding; WS-AWD = water-seeding + alternate wetting and drying; DS-AWD = direct dry seeding + alternate wetting and drying).

	$\delta^{15}\text{N-NO}_3^-$			$\delta^{15}\text{N-NH}_4^+$		
	DS-AWD	WS-AWD	WS-FLD	DS-AWD	WS-AWD	WS-FLD
$\delta^{15}\text{N-NO}_3^-$				-0.54*	-0.03	-0.05
$\delta^{15}\text{N-NH}_4^+$	-0.54*	-0.03	-0.05			
$\text{N}_2\text{O}_{\text{poreair}}$	0.34**	0.07	0.38**	-0.72***	0.04	0.22*
$\delta^{15}\text{N-N}_2\text{O}_{\text{poreair}}$	0.00	0.00	-0.14	0.46*	-0.03	0.14
NO_3^-	-0.66****	-0.01	-0.28	-0.41	0.11	0.27*
NH_4^+	0.01	0.13	-0.06	-0.54*	-0.23*	-0.12

5

Table 5. ANCOVA results of modeled residual N_2O not reduced (gross $r\text{N}_2\text{O}$), fraction of total $\text{N}_2 + \text{N}_2\text{O}$ production coming from denitrification (gross frac_{DEN}) and the fraction of N_2O attributed to denitrification (DenContribution) derived from $\text{N}_2\text{O}_{\text{emitted}}$ and $\text{N}_2\text{O}_{\text{poreair}}$. The Y position was used a co-variate and represents the longitudinal position of each replicate within field.

	NumDF	$\text{N}_2\text{O}_{\text{poreair}}$ $r\text{N}_2\text{O-gross}$	$\text{N}_2\text{O}_{\text{poreair}}$ $\text{frac}_{\text{DEN-gross}}$	DenContribution ($\text{N}_2\text{O}_{\text{poreair}}$)	NumDF	$\text{N}_2\text{O}_{\text{emitted}}$ $r\text{N}_2\text{O-gross}$	$\text{N}_2\text{O}_{\text{emitted}}$ $\text{frac}_{\text{DEN-gross}}$	DenContribution ($\text{N}_2\text{O}_{\text{emitted}}$)
treatment	2	0.004	<0.001	0.188	2	0.146	0.931	0.016
day	14	<0.001	0.001	<0.001	16	<0.001	<0.001	<0.001
depth	1	0.019	0.007	0.008				
Y position	1	0.844	0.016	0.375	1	0.451	0.373	0.818
trmt:day	28	0.001	<0.001	<0.001	19	0.009	0.024	<0.001
trmt:depth	2	0.330	0.082	0.052				
day:depth	14	0.185	<0.001	0.002				
trmt:day:depth	23	0.022	0.047	0.189				

10



Table 6. Spearman correlations between modeled rN_2O -gross, $frac_{DEN}$ -gross and $DenContribution$ with soil environmental variables and inorganic N substrates and $\delta^{15}N$ - N_2O . Results are for the mean of open and closed system dynamics. Subsurface correlations were performed on data aggregated across 5 and 12.5 cm depths. Significance indicated by: **** < 0.0001 , *** < 0.001 , ** < 0.01 , * < 0.05

5

	$frac_{DEN}$ -gross			rN_2O - gross			$DenContribution$		
	DS-AWD	WS-AWD	WS-FLD	DS-AWD	WS-AWD	WS-FLD	DS-AWD	WS-AWD	WS-FLD
<i>subsurface</i>									
$[N_2O_{poreair}]$	0.34***	0.2	0.31*	0.01	0.60****	0.17	0.67****	0.70****	0.59****
WFPS	0.21*	0.21*	0.39**	-0.11	0	-0.06	0.34***	0.22*	0.47***
Eh	-0.04	0.01	0.01	0.04	0.04	0.07	-0.03	-0.12	0.06
NO_3^-	0.16	0.01	0.16	0.13	0.15	0.04	0.28*	0.18	0.31*
NH_4^+	-0.22	-0.06	-0.19	0.21	0.41***	0.23	-0.06	0.33**	-0.03
$\delta^{15}N$ - $N_2O_{poreair}$	-0.35***	0.14	0.12	-0.03	-0.48****	-0.34**	-0.61****	-0.30**	-0.24
<i>surface</i>									
$[N_2O_{emitted}]$	-0.21	-0.73****	-0.40*	0.46***	0.77****	0.74****	0.64****	-0.11	0.27
WFPS	-0.12	-0.24	0.18	0.39**	0.29	0.1	0.60****	0.09	0.13
Eh	0.15	-0.22	0.08	-0.13	0.15	-0.17	-0.18	-0.39	-0.13
NO_3^-	-0.44**	-0.17	-0.28	0.32	0.19	0.31	0.19	0.06	0.01
NH_4^+	0.39*	0.52**	0.59**	-0.18	-0.58**	-0.51**	0.11	0.02	0.18
$\delta^{15}N$ - $N_2O_{emitted}$	0.60****	0.29	0.36	-0.80****	-0.33	-0.44*	-0.53****	0.19	-0.11